TECHNISCHE UNIVERSITÄT MÜNCHEN

Fakultät für Medizin

Yellow Fever Vaccination Induces the Short Form of Retinoic Acid-inducible Gene I in Human Mononuclear Cells

Livia Katharina Luciana Habenicht

Vollständiger Abdruck der von der Fakultät für Medizin der Technischen Universität München zur Erlangung des akademischen Grades eines

Doktors für Medizin

genehmigten Dissertation.

Vorsitzende(r):	Prof. Dr. Ernst J. Rummeny
Prüfer der Dissertation:	1. Prof. Dr. Anne Krug
	2. Prof. Dr. Dirk Busch

Die Dissertation wurde am 24.05.2016 bei der Technischen Universität München eingereicht und durch die Fakultät für Medizin am 15.02.2017 angenommen.

TABLE OF CONTENTS

I ZUSAMMENFASSUNG

In dieser Arbeit wurden Schlüsselparameter des Immunsystems in mononukleären Zellen des peripheren Bluts (peripheral blood mononuclear cells, PBMCs) von 13 gesunden Probanden im Alter von 22-32 Jahren vor und nach einer Impfung mit dem Gelbfieberimpfstoff YF-17D innerhalb eines Zeitfensters von 14 Tagen untersucht. Durch eine Kombination von quantitativer Reverse Transcription Polymerase Chain Reaction (qRT-PCR) und Western Blot Analysen wurde die Expression der Isoformen des Virussensors Retinoic-acid inducible gene RIG-I full length (RIG-I FL); RIG-I splice variant (RIG-I SV) und RIG-I short form (RIG-I SF), der Typ I Interferon (IFN)-induzierbaren Gene (ISGs) IRF7 (IFN regulatory factor 7; IRF7), ISG15 (ISG15 ubiquitin-like modifier; ISG15), MX1 (MX dynamin-like GTPase 1; MX1) und CXCL10 (C-X-C motif ligand 10; IP-10) untersucht. Zusätzlich wurde die Frequenz zentraler zirkulierender Immunzellen des angeborenen Immunsystems mittels Durchflußzytometrie bestimmt. Die mRNA der Typ I IFN ISGs *RIG-I, IRF7, ISG15, MX1* und *CXCL10* wurden an den Tagen 3 und 7 signifikant induziert und kehrten am Tag 14 zum Ausgangsniveau zurück; vor der Impfung (Tag 0) wurde das RIG-I FL Protein, nicht aber die RIG-I SV oder RIG-I SF Proteine, konstitutiv exprimiert. Am Tag 3 nach der Gelbfieberimpfung zeigte sich ein Anstieg der RIG-I SV und der RIG-I SF Proteine mit einem Gipfel der RIG-I SF am Tag 7 und einem anhaltend signifikant erhöhten Niveau dieser RIG-I Variante am Tag 14. Im Gegensatz zur Regulation von RIG-I zeigte sich bei der Regulation des Virussensors *melanoma differentiation-associated gene 5* (MDA5) Proteins eine Inhibition am Tag 3, 7 und 14, während für das Protein des Virussensors *laboratory of genetics and physiology 2* (LGP2) eine ähnliche

Kinetik wie bei RIG-I beobachtet werden konnte, d.h. eine Aufregulation an den Tagen 3 und 7 und eine Rückkehr zum Ausgangsniveau am Tag. 14. Die Prozentsätze der Monozyten und dendritischen Zellen (DC) innerhalb der PBMCs sowie der unterschiedlichen Monozyten und DC Subpopulationen wurden am Tag 0, 1, 3, 7 und 14 durchflusszytometrisch bestimmt. Zum Zeitpunkt 7 Tage nach der Impfung konnte in Korrelation mit der höchsten Expression der ISGs eine signifikante relative Reduktion der klassischen cluster of differentiation (CD) 14^+/$CD16^-$ Monozyten und ein signifikanter Anstieg der inflammatorischen $CD14^+$/$CD16^+$ Monozyten nachgewiesen werden. Weiterhin zeigte sich ein signifikanter Abfall der $CD141^+$ cDCs (konventionelle DCs) am Tag 3 und 7, während $CD1c^+$ cDCs am Tag 14 signifkant anstiegen und die plasmazytoiden DCs (pDCs) am Tag 14 deutlich abfielen. Außerdem konnte sowohl eine Aufregulation von HLA-DR als auch von CD86 bei $CD14^+$/$CD16^-$ und bei $CD14^+$/$CD16^+$ Monozyten und von HLA-DR bei $CD141^-$/$CD1c^+$ cDCs und von CD86 bei $CD141^+$/$CD1c^-$ cDCs nachgewiesen werden.

Die Ergebnisse der Arbeit zeigen, dass RIG-I FL konstitutiv in PBMCs nichtgeimpfter gesunder Probanden exprimiert wird und seine Expression sich während des Beobachtungszeitraums transient erhöht. Die Impfung mit dem Gelbfieberimpfstoff führt zu einer differentiellen Induktion der RIG-I SV und RIG-I SF Proteine, deren erhöhte Expression auch 14 Tage nach der Impfung, also über den Zeitpunkt der höchsten Expression der ISGs hinaus, anhielt. Da weder RIG-I SV noch RIG-I SF RNA Viren binden, sondern die Stimulation des Virussensors RIG-I durch virale RNA kompetitiv inhibieren, deuten diese Ergebnisse darauf hin, dass eine zu starke Typ I IFN Induktion durch die Induktion der endogenen Inhibitoren des RIG-I Signalwegs (RIG-I SV und RIG-I

SF) verhindert werden kann. Diese Daten zeigen erstmals, dass RIG-I SF durch die Gelbfieberimpfung *in vivo* induziert wird und deshalb als negativer Feedbackmediator von RIG-I FL agieren könnte. Durch die Ergebnisse wird die Hypothese unterstützt, dass in der frühen Immunantwort auf die Gelbfieberimpfung die Typ I IFN Antwort durch die Autoregulation des RIG-I Signalwegs kontrolliert wird. Bei Erkrankungen, die mit einer aberranten Regulation von Typ I IFN einhergehen, könnte die Induktion oder Suppression der RIG-I SF eine bisher unerkannte Interventionsmöglichkeit darstellen.

II SUMMARY

In this study, key parameters of the innate immune system were studied in peripheral blood mononuclear cells (PBMCs) of 13 healthy volunteers aged 22 to 32 years before and after vaccination against the yellow fever virus, i.e. YF-17D, during a time window of 14 days. Using a combination of quantitative reverse transcription polymerase chain reaction (qRT-PCR) analyses to determine the mRNA expression profiles of *DDX58* (RIG-I) itself and of several IFN-inducible genes (ISGs), Western blot analyses to measure expression of RIG-I full length (RIG-I FL), RIG-I splice variant (RIG-I SV), and RIG-I short form (RIG-I SF) proteins, together with fluorescence-activated cell sorting (FACS) analyses to examine alterations in the relative number of key innate immune cells in the circulation, the following results were obtained: qRT-PCR analysis revealed a marked and transient induction of RIG-I mRNA and of the type I ISGs, i.e. *IRF7* (IFN regulatory factor 7; IRF7), *ISG15* (ISG15 ubiquitin-like modifier; ISG15), *MX1* (MX dynamin-like GTPase 1; MX1), and *CXCL10* (C-X-C motif ligand 10; IP-10): mRNAs of IRF7, ISG15, MX1, and CXCL10 were markedly and transiently up-regulated on days 3 and 7 after vaccination, while their expression returned to baseline levels on day 14; Western blot analyses revealed that RIG-I FL protein but not its isoforms RIG-I SV or RIG-I SF, were constitutively expressed before vaccination and its expression level was further transiently enhanced during the observation period. Both RIG-I SV and RIG-I SF were induced on day 3 with RIG-I SF peaking on day 7 with a still markedly elevated level on day 14. In contrast to RIG-I, protein expression of *melanoma differentiation-associated gene 5* (MDA5) revealed inhibition at day 3 and thereafter though the protein of the virus sensor *laboratory of genetics and*

physiology 2 (LGP2) showed similar kinetics as RIG-I, i.e. induction at days 3 and 7 and return at day 14 to prevaccination levels. These data are the first to demonstrate that RIG-I SF is induced after yellow fever vaccination *in vivo*. The data are compatible with the hypothesis that both RIG-I SV and RIG-I SF are critical endogenous negative feedback regulators of the type I IFN response to prevent its toxic overexpression. FACS analyses revealed that the relative number of all mononuclear cells in the circulation did not show a significant change within 14 days after vaccination. The relative number of $CD14^+/CD16^-$ classical monocytes, however, was transiently down-regulated whereas the relative number of $CD14^+/CD16^+$ proinflammatory monocytes was significantly up-regulated on day 7. The relative number of all dendritic cells (DCs) remained unchanged during the course of the study. However, $CD141^+$ classical DCs (cDCs; the mouse homologue of $CD8^+$ DCs) were significantly reduced on days 3 and 7. In sharp contrast, $CD1c^+$ cDCs were elevated on day 3 and 7 whereas the relative number of plasmacytoid DCs (pDCs) among all DCs was markedly reduced on day 14. Moreover, we observed upregulation of HLA-DR and CD86 of $CD14^+/CD16^-$ and in $CD14^+/CD16^+$ monocytes and of HLA-DR in $CD141^-/CD1c^+$ cDCs and of CD86 in $CD141^+/CD1c^-$ cDCs. In summary, these data reveal that both RIG-I mRNA and RIG-I FL protein are constitutively expressed in young healthy individuals before vaccination with significant transient changes during the observation period after immunization. Moreover, vaccination led to a significant upregulation of RIG-I mRNA and their respective proteins though RIG-I SF remained markedly elevated on day 14. Furthermore, vaccination was associated with significant upregulation of a series of classical ISGs. These data show that yellow fever vaccination in healthy young adults is associated with significant upregulation of ISGs and their cellular constituents in

a scenario to ensure strong IFN responses while restricting toxic and overshooting responses at later time points. Although the regulation of RIG-I is arguably complex, the data obtained in this study indicate that RIG-I SV and RIG-I SF may represent hitherto unrecognized physiologically important negative feedback regulators of the type I IFN response. These data open the possibility to test new therapeutic strategies in diseases with aberrant type I IFN responses to either promote or to inhibit expression of RIG-I SF.

INDEX OF FIGURES

INDEX OF TABLES

ABBREVIATIONS

AA	Amino acid
APS	Adenosine 5'-Phosphosulfate
ATP	Adenosine 5´-triphosphate
BCRs	B cell receptors (antigen-recognizing)
CARD	Caspase activation and recruitment domain
CARDIF	CARD adapter inducing IFN-β
CTD	C-terminal domain
CXC family	C-X-C family of chemokines
CXCL10	C-X-C motif ligand 10
CXCR	C-X-C receptor
cDC	Conventional dendritic cell
CTD/RD	C-terminal regulatory domain
DC(s)	Dendritic cell(s)
DC-medium	Dendritic cell medium
ds	Double stranded
DDX58	DEAD (Asp-Glu-Ala-Asp) Box Polypeptide 58
DNA	Desoxoyribonucleic acid
DMSO	Dimethyl sulfoxide
EBV	Epstein–Barr virus
EDTA	Ethylenediaminetetraacetic Acid
EtOH	Ethanol
FACS	Fluorescence-activated cell sorting
FADD	Fas associated via death domain
FCS	Fetal calf serum
FL	Full length
GTP	Guanosine triphosphate metabolizing protein
HCL	Hydrochloric acid
HCV	Hepatitis C virus
HEK 293 cells	Human embryonic kidney cells
Hel1	Helicase domain 1
Hel2	Helicase domain 2
HLA-DR	Human leukocyte antigen-D related
IFN-β	Interferon β
IKK-i-dependent	IKBKE inhibitor of kappa light polypeptide gene enhancer in B-cells, kinase epsilon
IP-10	Interferon inducible protein 10
IPS-1	IFN-β promoter stimulator 1
IRF7	IFN regulatory factor 7
ISGs	IFN-stimulated genes
ISG15	ISG15 ubiquitin-like modifier
JeV	Japanese encephalitis virus
kDa	Kilodalton
LGP2	laboratory of genetics and physiology 2
MAMPs	microorganism-associated molecular patterns
MAVS	Mitochondrial antiviral signaling protein
MDA5	melanoma differentiation-associated gene 5
Min	Minute
mM	Millimolar

mRNA	Messenger RNA
MX1	MX dynamin-like GTPase 1
NAP1	CXCL8 chemokine (C-X-C motif) ligand 8
NDV	Newcastle disease virus
NEMO	IKBKG inhibitor of kappa light polypeptide geen enhancer in B-cells, kinase gamma
NFκB	Nuclear factor-κB
NOD	Nucleotide oligomerization domain
NP40	Nonylphenolethoxylat P-40
PAMPs	Pathogen-associated molecular patterns
PBMCs	Peripheral blood mononuclear cells
PBS	Phosphate buffered saline
PCR	Polymerase chain reaction
pDC	Plasmacytoid DCs
pH	Power of hydrogen
PMFS	Phenylmethylsulfonylfluorid
5´ pppRNA	5´ triphosphate RNA
pppVSVL	Specific ligand 5´-triphosphate RNA
PRR(s)	Pattern recognition receptor(s)
µl	Microliter
qRT-PCR	Quantitative reverse transcription polymerase chain reaction
RD	Regulatory domain
RIG-I	Retinoic acid inducible gene I
RIP-1	RIPK1 receptor interacting serine/threonine kinase 1
RLRs	RIG-I like receptors
RNA	Ribonucleic acid
rpm	Revolutions per minute
RSV	Respiratory syncytial virus
RT	Room temperature
RT-PCR	Reverse transcriptase PCR
SDS-PAGE	Sodium dodecyl sulfate polyacrylamide gel electrophoresis
SEM	Standard error of the mean
SeV	Sendai virus
SF	Short form
SV	Splice variant
TBK1	TANK-binding kinase 1
TBS-T	Tris buffered saline with Tween-20
TANK	TRAF family member-associated NFκB activator
TCRs	Antigen-recognizing T cell receptors
TEMED	Tetramethylethylenediamine
TLRs	Toll-like receptors
TNF	Tumor necrosis factor
TRADD	TNF receptor-associated death domain
TRAF	TNF receptor-associated factor
TRIS	Tris (hydroxymethyl) aminomethan
VISA	Virus-induced signaling adapter
YF-17D	Yellow fever-17D

1 INTRODUCTION

The Innate and Adaptive Immune Systems

Since the beginning of immunology in 1796, when Edward Jenner discovered vaccination against human smallpox, the immune system has been viewed as being divided into two major separable entities, i.e. the innate and the adaptive immune systems, which have to protect us from invading pathogens such as bacteria, funghi, and viruses. Innate immune cells are activated within seconds to minutes while the adaptive immune system requires days to months until its forces are put into full action. Therefore, innate immunity is the first line of defense against invading pathogens (Iwasaki and Pillai, 2014). Its cellular constituents include neutrophils, monocytes/macrophages, eosinophils, mast cells, and several DC subtypes. These cells interact with non-hematopoietic cells such as endothelial cells or epithelial cells to rapidly migrate towards the pathogen. The pathogen is then killed or attenuated by a series of intricate mechanisms including phagocytosis, complement-mediated target cell injury, or otherwise damaged by the immune cells´ secretion products. For example, type I IFNs (IFNα, IFNβ) play major roles as mediators of antiviral activities exerted by innate immune cells including monocytes and DCs but also by non-immune cells (Eisenächer and Krug, 2012).

In contrast, adaptive immunity is characterized by delayed responses that are carried out by B (Kurosaki et al., 2015; Browning, 2006; Shen and Fillatreau, 2015) or T lymphocytes (Geginat et al., 2001; Mackay, 1999). B cells conduct humoral immunity by the production of antibodies though they are also involved

in cytokine production and regulatory tasks towards T cells. T cells have a wide range of activities including target cell killing and T cell help through synthesis and secretion of a variety of cytokines. Moreover, regulatory T cells inhibit effector T cell responses and maintain peripheral tolerance (Sakaguchi et al., 2013).

While innate immune cells recognize pathogens via pattern recognition receptors (PRRs) with broad binding characteristics, lymphocytes recognize short peptides or lipid moieties (called “epitopes”) derived from processed proteins, lipids or other molecules in a highly specific way. PRRs on innate immune cells are germline-encoded while lymphocyte antigen receptors are acquired after birth. B cells are equipped with antigen-recognizing BCRs, which are the molecules that provide humoral immunity through antibody production, whereas T cells with their antigen-recognizing T cell receptors (TCRs) provide cellular immunity. BCRs of memory B cells or plasma cells develop through sequential hypermutation of the variable regions of immunoglobulins and further mutations termed affinity maturation in germinal centers of secondary lymphoid organs such as lymph nodes and spleen. The resulting B cell receptor (BCR) repertoire yields an enormous number of clonal B cells each carrying a specific BCR that is capable of responding to an antigen-epitope. In addition, T cells carrying T cell receptors (TCRs) develop in the thymus where a comparably large number of T cells is generated, that are likewise directed towards antigen epitopes, forming the TCR repertoire. However, extrathymic T cells, unlike their B cell counterparts, do not or to a much lesser extent undergo hypermutation and affinity maturation. Instead, T cells undergo a maturation pathway referred to as avidity maturation after their TCR repertoire has been established in the

thymus. DCs bridge the innate and the adaptive immune systems by presenting antigens as peptide sequences bound to major histocompatibility complexes class I and II (Palucka and Banchereau, 2013; Meixlsperger et al., 2013; Steinman, 2012; Lanzavecchia and Sallusto, 2011). Moreover, different DC subtypes are involved in cytokine production and regulatory functions of distinct steps of an antigen-dependent immune response (Zhang et al., 2015; Swiecki and Colonna, 2015). When taken together, recognition of pathogens by innate and adaptive immune cells plays sequential roles to eliminate the antigen. Accordingly, studies of PRRs, BCRs, and TCRs have moved onto the center stage of immunity research.

Monocytes, Macrophages, and DCs: Gatekeepers of Innate Immunity

Central to this clinical study in humans on yellow fever vaccination is the analysis of major cellular constituents of innate immune cells, i.e. monocytes and DCs collectively referred to as the mononuclear phagocyte system (Guilliams et al., 2014; Gordon and Taylor, 2005). Each of the immune cell subtypes of the mononuclear phagocyte system constitute a group of heterogeneous mononuclear cells whose nomenclature and precise designation varies depending on their ontogeny, marker expression, function within the immune system, and the species they are derived from (Geissmann et al., 2010). The common feature of the members of the mononuclear phagocyte system is that they exist in a quiescent state under normal conditions of immune homeostasis and that they are activated by what has been termed “danger signals” to acquire capabilities to bind and process the dangerous invader, adopt migratory characteristics, and differentiate into effector cells. During

differentiation, each MPS member becomes highly skilled in various capacities such as phagocytosis, antigen presentation to T and B cells, distinct responses to microbes, cytokine and chemokine patterns they secrete, and mediation of tolerance (Shortman and Liu, 2002; Kapsenberg, 2003). It is important to point out that virus invasion threatens the life of the host within hours and that the mononuclear phagocyte system has two separate tasks to deal with that danger in a very short time window: First, cells of the MPS need to sense, then mount a robust immediate innate immune response. This task is largely carried out by distinct monocyte subtypes and tissue macrophages including the $CD14^+/CD16^-$ classical monocytes and the $CD14^+/CD16^+$ inflammatory monocytes (Ziegler-Heitbrock, 2015; Ziegler-Heitbrock, 2007). When the immune system senses a systemic danger as in yellow fever infections, further cells are mobilized from the bone marrow. Secondly, the mononuclear phagocyte system needs to provide the molecular mechanisms to prepare the adaptive immune system to not only recognize the danger but begin to initiate a longlasting protective adaptive immune response in B and T cells without attacking the host tissue (Altfeld and Gale Jr, 2015). The latter tasks are largely carried out by DC subtypes. Moreover, some DC subtypes are derived from circulating monocytes to differentiate into antigen-presenting DCs. Tasks of the DC subtypes are also initiated early and involve complex forward responses including generation of cytokines, chemokines, and IFNs, and respective negative feedback loops. Human DCs constitute a heterogeneous group of DCs with very different functions. The major task of $CD1c^+$ DCs is to activate T helper cells. $CD141^+$ cDCs are major cross-presenting DCs whereas pDCs are major IFN-producing cells and - upon activation of TLRs - activate T cells (Beignon et al., 2003; Cella et al., 2000; Swiecki and Colonna, 2015; Shakhar et al., 2005).

Pattern Recognition Receptors (PRRs)

Structures of pathogens such as lipoprotein moieties of cell walls of bacteria and sequences of DNA or RNA resemble each other to a certain extent. These broadly recognized structures are called pathogen-associated molecular patterns (PAMPs). PAMPs are detected by PRRs as nonself through their surface receptors such as Toll-like receptors (TLRs) either on the surface or in the cytosol of innate immune cells. However, it became evident that non-pathogenic and indeed commensal bacterial strains that make up the gut microbiota also activate PRRs (Barbalat et al., 2011; Brubaker et al., 2015). Therefore the PAMPs are more appropriately called microorganism-associated molecular patterns (MAMPs), because under physiological conditions they endow beneficial rather than pathological activities to the host (Swiecki and Colonna, 2015). Interaction of PAMPs or MAMPs with PRRs subsequently activate innate immune cells resulting in the initiation of a variety of signaling cascades that ultimately lead to immune responses of various effector mechanisms such as phagocytosis or secretion of distinct cytokine patterns to eliminate the invading pathogen. Unlike the TCRs or BCRs, PRRs are germline-encoded and cannot react to specific antigen derminants but rather respond to broad patterns that are found in many invading organisms. This has the advantage that they respond quickly without the need to adapt through postnatal gene modifications. PRRs can be divided into subgroups including TLRs, C-type lectin receptor, NOD-like receptors, and retinoic acid gene I-inducible (RIG-I)-like receptors (RLRs). We will focus below on the RLR family (Stuart et al., 2013), which are critically involved in innate antiviral immune defenses.

The Family of RIG-I-like Receptors (RLRs)

Three members of RLRs have been identified: RIG-I, MDA5, and LGP2 (Iwasaki and Pillai, 2014; Goubau et al., 2013; Rehwinkel and e Sousa, 2013; Pulendran et al., 2013; Schlee, 2013). It is well established that RLRs play a major role in the detection and restriction of viral infections by their ability to detect RNA or DNA sequences derived from replicating viruses (Fig. 1). Unlike the surface TLRs, RLRs are exclusively located in the cytosol. RLRs are part of the DExD/H-box helicase family (Fig. 2). Each of the three RLRs possesses two helicase domains (Hel1 and Hel2). The helicase domains are flanked by a C-terminal regulatory domain (CTD/RD) and by a tandem caspase activation and recruitment domain (CARD) at the N-terminus of RIG-I and MDA5, a domain, which is lacking in LGP2 (Fig. 1). The involvement of LGP2 in sensing of viral RNA is less well understood, in contrast to the better known MDA5 and RIG-I.

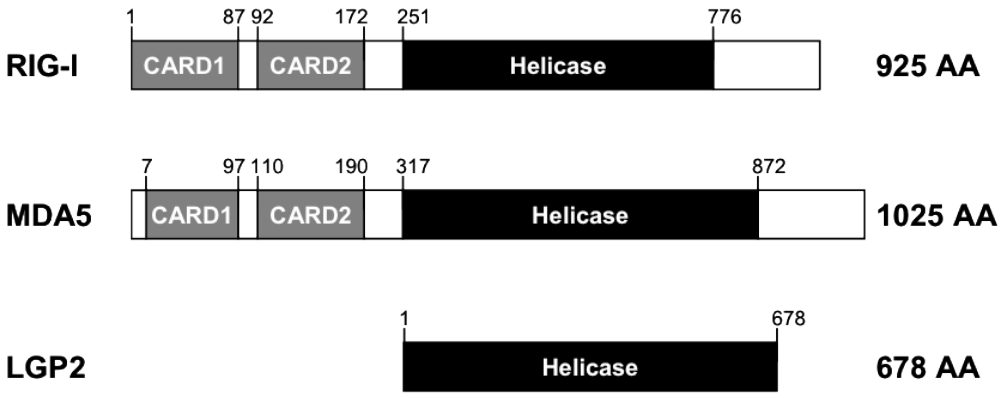

Fig. 1. Domain structure of RLR family members: RIG-I, MDA5, and LGP2. Reproduced from Eisenächer: "Functional analysis of cytosolic sensors of viral nucleic acids and their role for innate antiviral immune defense." Doctoral Thesis Katharina Eisenächer (2011).

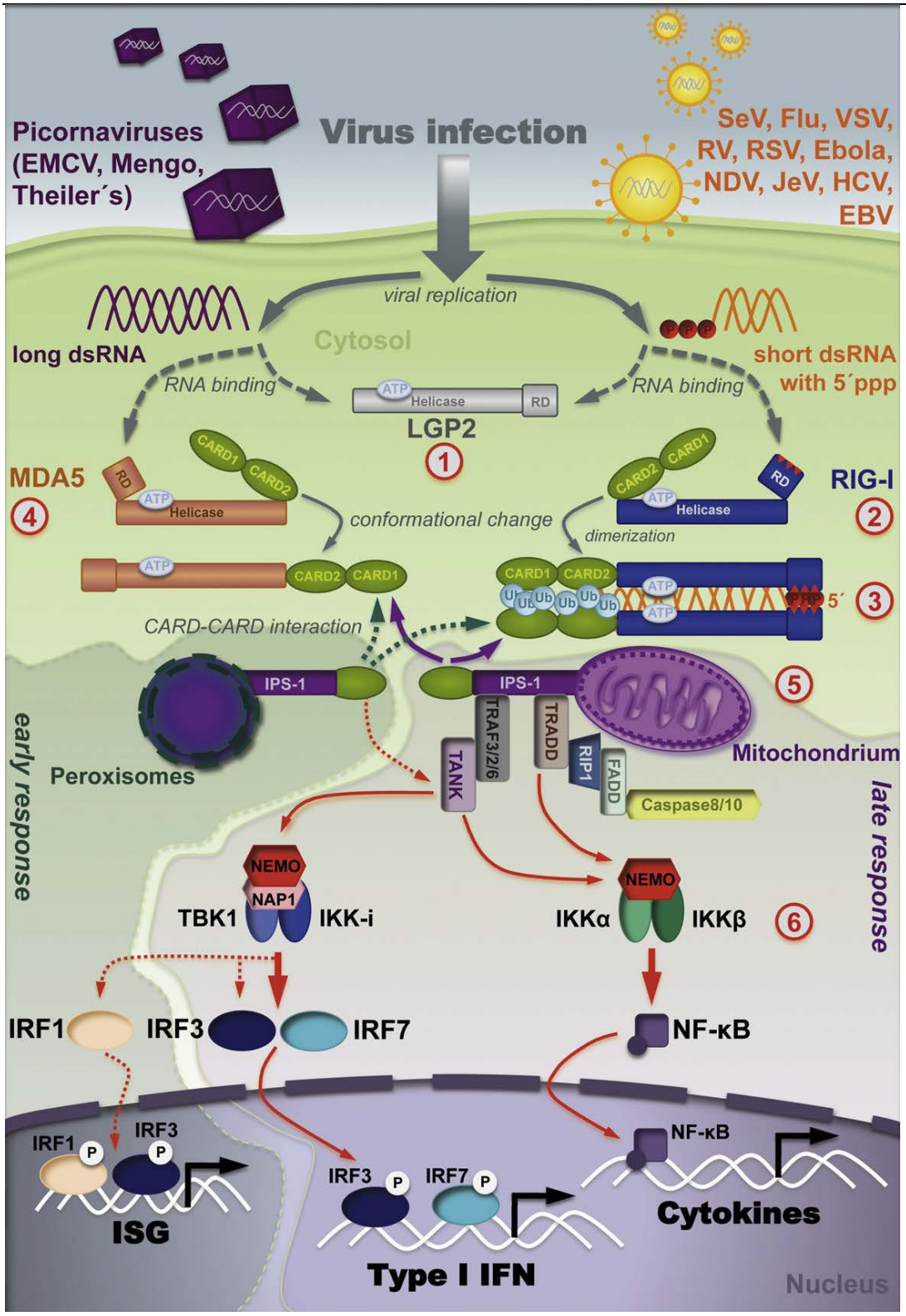

Fig. 2. RLR-mediated signal transduction and its regulation. RIG-I and MDA5 exert differential roles in the recognition of RNA viruses. While RIG-I recognizes various types of RNA viruses, such as Sendai virus (SeV), influenza, vesicular stomatitis virus (VSV), respiratory syncytial virus (RSV), Ebola virus, Newcastle disease virus (NDV), Japanese encephalitis virus (JeV), hepatitis C virus (HCV) and Epstein–Barr virus (EBV), MDA5 is specifically activated by members of the picornavirus family. Upon virus infection, long viral dsRNA or short 5_-triphosphorylated RNA (5_pppRNA) activates MDA5 or RIG-I, respectively, by binding to their C-terminal regulatory domains (RD), which contain a leucine-rich basic cleft that mediates binding of the negatively charged RNA and confers ligand specificity. A positively charged triphosphate-binding groove within the RD of RIG-I specifically binds the RNA 5_-triphosphate.

LGP2 also binds dsRNA by its RD and functions as a positive regulator in both RIG-I and MDA5-mediated virus recognition. Once activated, RIG-I undergoes an ATP-dependent conformational change that promotes dimerization and exposure of the CARDs, leading to subsequent interaction with the common signaling adapter IPS-1 via homotypic CARD–CARD binding. Mitochondrial IPS-1 then triggers the expression of type I IFN genes by activating TRAF3/2/6, TANK and NEMO/NAP1, resulting in TBK1/IKK-i-dependent activation of IRF3/7. Simultaneously, mitochondrial IPS-1 signaling induces nuclear translocation of NF-_B via TRADD and the RIP-1/FADD/caspase8/10 complex. Recently, it was shown that IPS-1 localized to the peroxisomes mediates rapid IRF1/3-dependent expression of IFN-stimulated genes (ISGs), which induces an early, but transient antiviral response that is independent of type I IFN. This early antiviral state limits the infection until enough IFN is produced to trigger the expression of a complete panel of ISGs and to halt viral replication, permanently. To prevent uncontrolled immune responses, RLR signaling is regulated by various mechanisms at multiple steps of the signaling cascade: (1) LGP2 acts as a positive regulator for RIG-I and MDA5 signaling; (2) autoregulation of RIG-I activity by the RD and RIG-I splice variant; (3) posttranslational modification of RIG-I: ubiquitination, ISGylation, phosphorylation; (4) dihydroxyacetone kinase (DAK) keeps MDA5 inactive in the steady state; (5) regulation at the level of the RLR–IPS-1 axis; (6) modulation of RLR signaling by targeting downstream molecules (Reproduced from Eisenächer and Krug; Regulation of RLR-mediated innate immune signaling – it is all about keeping the balance. European Journal of Cell Biology 91 (2012); 36-47).

(Iwasaki and Pillai, 2014; Pulendran et al., 2013; Rappuoli et al., 2011). RLRs sense viral RNA. However, although several mechanisms have been identified, the molecular mechanisms how RLRs distinguish between self and non-self RNA is an ongoing field of interest in immune response research: Generally, RLRs have the capability to recognize components of RNA viruses (Eisenächer and Krug, 2012; Kell and Gale, 2015; Chan and Gack, 2015b). Following virus uptake (of hepatitis virus, Ebola virus, EBV and others) into the cytosol of innate immune cells and its replication, the specific ligand domain for RIG-I is a short dsRNA sequence with a triphosphate moiety at the 5´-end (Hornung et al., 2006). In contrast, the RNA of picornaviruses such as Theiler´s virus and the Mengo virus, bind to MDA5 and LGP2 as long double stranded RNA sequences without a phosphate moiety attached. These differential binding characteristics provide virus-specificity within the RLR family of cytosolic sensors although LGP2 can bind both Picornavirus RNA and short double-stranded RNA sequences with a phosphate moiety attached. The specificity of RIG-I or MDA5 to sense specific virus-derived RNA sequences without or with phosphate

groups is located in their distinct RNA binding domains (Eisenächer and Krug, 2012) while both share a common downstream signaling pathway (Fig. 1). The signaling cascades of both RIG-I and MDA5 lead to the activation of the transcription factors IFN regulatory factor (IRF) 3 and 7 and of nuclear factor-κB (NFκB), which once activated translocate to the nucleus where they bind to their respective promoter regions to induce expression of type I IFN as well as proinflammatory cytokines. Although it is beyond the scope of this study, a few principal components of the RIG-I signaling cascade deserve attention as summarized in Fig. 1. Recognition of viral PAMPs or MAMPs by the C-terminal RD of RIG-I and MDA5 induces conformational changes within their respective receptor binding domains. Mutant RIG-I lacking the caspase activation and recruitment domains (CARDs) is not able to initiate a downstream signaling cascade (Yoneyama et al., 2004). Following binding of viral RNA to an RLR, a conformational change results in the initiation of the RLR signaling cascade. The receptor domains become activated in a way that the CARDs are now able to communicate with the adaptor protein IFN-beta promoter stimulator 1 (IPS-1; also known as MAVS; CARDIF; VISA) (Fig. 1) (Seth et al., 2005; Wu and Hur, 2015; Belgnaoui et al., 2011). Through interactions with various kinases and activation and translocation of IRF-3/7 and NF-κB into the nucleus (which act as transcription factors), a type I IFN response and the production of inflammatory cytokines is triggered at the transcriptional level. Subsequently, ISGs propel the cell into an antiviral state. This allows the innate immune cells such as a monocytes/macrophages to perform three major tasks: First, through phagocytosis and cytokine secretion, the immune cells will be capable of eliminating the pathogen; second, through the production of type I IFNs, they directly inhibit virus replication; and third, it becomes a focus to attract

lymphocytes through chemotactic mediators. The resulting linkage of the innate and adaptive immune systems allows to trigger a vigorous humoral immune response by B cells to produce antiviral antibody responses (Stuart et al., 2013). However, although much has been learned during recent years, i.e. their main activities to induce a type I IFN response, understanding the molecular mechanisms of RIG-I and MDA5 activities including their negative feedback regulation to prevent harmful tissue responses for the host and their relevance towards mediating adaptive immune responses in B and T cells in human diseases and in vaccinations strategies are not fully understood (Fig. 1 and see below).

RIG-I Full Length (RIG-I FL)

RIG-I is the most intensively studied receptor of the family of the three RLRs and therefore the best understood. After recognition of the viral RNA, RIG-I activates a signaling cascade resulting in the production of type I IFNs. IFNs not only support an antiviral state but also increase the expression of RIG-I in a positive feedback loop due to the IFN-inducible nature of the RIG-I gene (Chan and Gack, 2015b). RIG-I Regulation of RIG-I is complex but ubiquitination seems to be important leading to RIG-I regulation (Chan and Gack, 2015b). However, additional posttranslational modifications including phosphorylation and ISGylation and deISGylation cycles play additional roles (Gack et al., 2008). As pointed out above, RIG-I and MDA5 can distinguish various RNA ligands, but the downstream signaling cascade is similar. CARDs act as effector domains that inititate downstream signaling. CARD1-CARD2 interact with adapter proteins designated as IFN-β promotor stimulator 1 (IPS-1 also referred to as mitochondrial antiviral signaling molecule, MAVS; virus-induced signaling

adapter, VISA; CARD adapter inducing IFN- β) leads to activation of the NF-κB translocation from the cytosol to the nucleus and the activation of NF-κB-inducible cytokines or to the activation of IRF3/7 with subsequent induction of type-I IFN (Fig. 1). Moreover, RIG-I is not only a sensor of viral RNA but appears to function as a direct antiviral factor for hepatitis B virus by blocking virus replication in the cytosol independent of its signaling (Chan and Gack, 2015a; Sato et al., 2015). RIG-I seems to be further regulated by its own splice variant (SV) (Chiang et al., 2014) as described below.

RIG-I Splice Variant (RIG-I SV)

RIG-I SV has been identified as a negative regulator of its own pathway (Gack et al., 2008; Gack et al., 2010). It lacks a short amino acid sequence (AA 36 to 80 within exon 2) in its first CARD which results in interference of protein interactions required for signaling. Expression of RIG-I SV is increased after viral infection and/or IFN-β treatment *in vitro* (Honda et al., 2006; Loo and Gale, 2011). It is therefore conceivable to assume that RIG-I SV prevents an overshooting IFN response, which would harm the cell and have injurious effects on the surrounding tissue. However, RIG-I SV is only transiently expressed (Fig. 3).

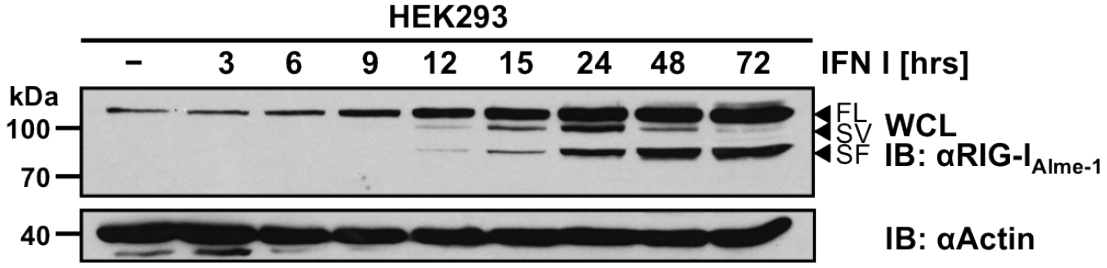

Fig. 3. Regulation of RIG-I FL, RIG-I SV, and RIG-I SF proteins in HEK293 cells stimulated with IFN I. Reproduced from Eisenächer: "Functional analysis of cytosolic sensors of viral nucleic acids and their role for innate antiviral immune defense." Doctoral Thesis Katharina Eisenächer (2011).

Discovery of RIG-I Short Form (RIG-I SF)

A hitherto unknown short isoform of human RIG-I (in the following referred to as RIG-I SF) has been discovered in our group (unpublished data). Using two monoclonal antibodies, Alme-1 directed against amino acids 201-713 (Helicase domain) and 8G7-12 directed against amino acids 905-925 (CTD), three (instead of the expected two) bands were detected by Western blot analyses of whole cell lysates of HEK293 cells that had been stimulated with 1000 U/ml type I IFN: The two known RIG-I members, i.e. RIG-I full length (RIG-I FL) of 106 kDa and its splice variant, i.e. RIG-I SV (DDX58 isoform 2, UniProt entry O955786-2) of 101 kDa. In addition to the two known RIG-I proteins, however, a third band of approximately 95 kDa was seen in IFN-stimulated but not in unstimulated cells (Fig. 3). Mass spectrometry analyses revealed that this band contained a short isoform of RIG-I (RIG-SF), which is truncated at the N-terminus lacking CARD1 and parts of CARD2. Functional analysis of this isoform showed that it signaling defective and inhibits RIG-I activation by its ligand (unpublished results). Thus, the short form of RIG-I is an endogenous novel negative feedback regulator of RIG-I-mediated IFN-β production. These *in vitro* findings led to the important question of how all three RIG-I forms may be regulated *in vivo*. In particular, to further examine its physiological significance, it became mandatory to determine whether RIG-I SF may also be inducible *in vivo*. Moreover, these data raise new questions how and which innate immune cells respond to a prototypic viral infection (Rappuoli et al., 2011).

YF-17D Vaccination: A Model for the Impact of Yellow Fever Virus Infection on the Immune System *In Vivo*

Vaccinations against viruses are of immeasurable clinical importance due to the high death rate viruses cause worldwide (Rappuoli et al., 2011). Yellow fever is a severe viral infectious disease caused by the mosquito-borne yellow fever virus of the Flavivirus family. The RNA virus has several important structural features each of which contribute to its virulence including binding and uptake by plasma membranes (capsid protein C), initiation of infection (E proteins which are also antigen epitopes important for vaccination), nonstructural protein 1 (NS1) believed to regulate replication, and the NS2A protein involved in packaging and replication of the virus. Yellow fever can lead to haematemesis, failure of various organs including kidney, liver, and heart. 50% of all cases are lethal in nonvaccinated individuals (Pulendran, 2009). Currently there are no medications available that are powerful enough to repress the infection. These data show the enormous importance of yellow fever vaccination. Therefore, the World Health Organisation recommends people traveling to sub-Saharan Africa, tropical regions of South America (Pulendran, 2009) and other endemic yellow fever regions, to get vaccinated against the yellow fever virus. The efficiency of the life virus vaccine using the YF17D attenuated vaccine strain, is higher than 90% (Pulendran et al., 2013). Recent studies on adverse events in eight African countries support the safety of yellow fever preventive vaccination strategies as suggested by the World Health Organization (Breugelmans et al., 2013). In a total population of 38 million people, 22 people showed presumptive yellow fever vaccination reactions. Only 6 of the 22 developed yellow fever vaccine-associated neurologic disease. The production of the vaccine is carried out in embryonated chicken eggs and thus is contraindicated in people allergic against

egg components. Other side effects such as influenza-like symptoms, nausea, diarrhea, and myalgia are possible (http://www.who.int/ith/vaccines/yf/en/). Otherwise the vaccine, i.e. YF-17D, is well tolerated as evidenced by its use in more than 500 million people. Indeed, it is now known as one of the oldest and most successful vaccines ever produced. Its success has been honored with the Nobel Prize for Medicine or Physiology in 1951 to Max Theiler (Pulendran, 2009).

Due to the fact that the yellow fever vaccine is well understood and widely administered it has been used as an archetype tool to perturb and study the immune system in response to virus infection in humans *in vivo*. Unlike influenza virus infection, which is widely endemic in our population, yellow fever vaccination provides a model in humans that is suitable to study a primary immune response, i.e. it investigates the immune system that has never been exposed to yellow fever viral antigens. Moreover, it allows the study of the immune system in a synchronized way so that the kinetics of changes in the innate and adaptive immune responses can be readily investigated after vaccination by using easily accessible blood cells. Consequently, different studies have been carried out in mice as well as in humans: Thanks to yellow fever vaccination studies there is now an enormous body of data from which immunologists have learned, how the immune system responds to prototypic virus infection. From this data, it is apparent that yellow fever vaccination has become a paradigm of other viruses afflicting humans (Pulendran et al., 2013). Understanding the mechanisms of how the vaccine works not only helps to introduce even better vaccines but also advances our understanding of the immune system towards other virus infections. The attenuated YF-17D virus

replicates *in vivo* (see above). Peak viral titers are detected in the serum on day 7 postinjection. Vaccination triggers a robust type I IFN response and concomitantly expression ISGs (Gaucher et al., 2008; Querec et al., 2009). Yellow fever virus YF-17D vaccination is therefore a suitable model for the study of type I IFN responses in humans. Thus, understanding the mechanisms of yellow fever vaccination immunity will undoubtedly yield important new therapeutic strategies in diseases as diverse as chronic inflammation, cancer immunity, and autoimmune diseases in the future.

Aims of the Project

Yellow fever vaccination was chosen as a well established model to study the innate immune response to a replicating RNA virus *in vivo* in humans. The vaccine is life-attenuated and consequently actively replicates *in vivo*. (Pulendran et al., 2013). By vaccinating healthy women and men aged 22 to 32 we set out to delineate key components of the immune response *in vivo*. In particular, I focused my attention on RIG-I and its novel short isoform, which seems to play a role as potent negative feedback regulator of the RIG-I-dependent type I IFN response. In this study we chose five time points: Day 0 (before vaccination), day 1, day 3, day 7, and day 14 after vaccination. We assumed that this time window would allow us to possibly observe alterations in key cells of the innate immune system and the initial changes in the adaptive immune system. The aim of my thesis was to study the expression of RLRs, in particular RIG-I and its regulatory isoform, after YF17D vaccination and to correlate this with the type I IFN gene signature and the frequency of monocyte and DC subpopulations in the blood.

2 MATERIALS AND METHODS

Materials

Human Blood Samples

The study was approved by the ethics committee oft the Technical University Munich. Signed consent was obtained from study participants before enrollment. Participants included into the study had planned to travel to a country at risk of yellow fever transmission and therefore needed the vaccination for disease prevention. Health care professionals at the Institute for Tropical Medicine of the Ludwig-Maximilians-Univeristy of Munich and the II Department of the University Hospital of the Technical University of Munich (Klinikum Rechts der Isar) drew venous blood from 13 healthy volunteers aged between 22 and 32 (see Tab. 10. in Results below). For this purpose, BD-Vacutainer Safety-Lok Blood Collection Sets (anticoagulant: ACD – Acid Citrate Dextrose/Glucose) with pre-attached holders and BD-Vacutainer tubes were used to collect a total of 55 ml blood per withdrawal from each volunteer. Blood samples were transported to the laboratory for immediate processing at room temperature (RT).

Yellow Fever Vaccine

The yellow fever vaccine used in this study was STAMARIL (Sanofi Pasteur MSD) containing the YF17D vaccine strain. YF-17D is a life-attenuated vaccine of the yellow fever virus 17D-204 strain. One dose of the vaccine (0,5 ml)

contains at least 1000 LD_{50} units[2] 17D-204. Vaccination was performed as described by the manufacturer subcutaneously.

Standard Solutions and Buffers

Solution	Composition	Storage
Biocoll separating solution	Composition as described by the manufacturer: Biochrom – Isotonic solution – Density 1.077 g/ml	RT
PBS	Dulbecco´s PBS (1x) without Ca^{2+} and $Mg2^{+}$ – sterile	RT/4° C
Red blood cell lysing buffer (Sigma-Life Science: R775)	0,83% ammonium chloride in 0,01 M Tris buffer	RT
DC-Medium	RPMI Promocell 10% fetal calf serum 1% penicillin/streptomycin 1% non-essential amino acids 1% sodium pyruvate 1% glutamax 0,05 mM β-ME (mercaptoethanol)	4° C

Tab. 1. Standard solutions and buffers for the isolation of PBMCs.

Solution	Composition	Storage
DMSO	Dimethyl sulfoxide	RT
FCS	Fetal calf serum	RT/4° C
Freezing Medium	90% DMSO	4° C

	10% fetal calf serum	

Tab. 2. Standard solutions and buffers for cryopreservation of PBMCs.

Solution	Composition	Storage
PBS	Dulbecco´s PBS (1x) without Ca^{2+} and $Mg2^{+}$ – sterile	RT/4° C
Western blot lysis buffer	10 % Glycerol 20 mM Tris- HCl pH 7 137 mM NaCl 2 mM EDTA 1% NP40 (Igepal) in distilled water In 10 ml aliquots 1 tablet complete mini protease inhibitor diluted + 100 µl PMSF (100 mM) + 20 µl sodium orthovanadate (500 mM)	4° C

Tab. 3. Standard solutions and buffers for Western blot lysate preparation from PBMCs.

Solution	Composition	Storage
Trizol	Composition as described by the manufacturer: Ambion/RNA by life technologies	4° C

Tab. 4. Standard solutions and buffers for RNA Trizol preservation.

Solution	Composition	Storage
Separation Gel	Polyacrylamide 3,3 ml (Rotiphorese®	4° C

	Gel 30 (37,5:1; Roth)) Lower sample buffer 2,5 ml Distilled water 4,1 ml APS (10%) 0,1 ml TEMED 3,3 µl	
Collection Gel	Polyacrylamide 2,5 ml (30%) Upper sample buffer 3,75ml Distilled water 9,75ml APS (10%) 100 µl TEMED 20 µl	
TBST	Tris-HCl (1 M pH 8,0) NaCl (150 mM) Tween 20 (0,05%) (1 ml 50% Tween-solution) Add 1 liter distilled water	RT
Blocking Solution	5% Skim milk powder in TBST	RT
Transfer Buffer (semi dry method)	Tris 5g Glycin 28,8 g MetOH 400 ml Add 2 liter distilled water	RT
Western Blot Lysis Buffer	10 % Glycerol 20 mM Tris-HCl pH 7.0 137 mM Sodium chloride 2 mM EDTA 1 % NP-40 in distilled water the following supplements were added freshly prior to use:	4° C

	1 tablet complete protease inhibitor mix 100 µl 100 mM PMSF (in Methanol) 20 µl 500 mM Sodium orthovanadate (in ddH_2O) in 10 ml IP lysis buffer	
10x Lämmli Sample Buffer	Glycin 288 g Tris 60,6 g SDS 30 g Add 2 liter distilled water	RT
4x Upper Sample Buffer (pH 6,8)	0,5 M Tris 33 g 0,4% SDS 10 ml (20%) Add 500 ml distilled water	RT
4x Lower Sample Buffer (pH 8,8)	1,5 M Tris 90,85 g 0,4% SDS 10 ml (20%) Add 500 ml distilled water	RT

Tab. 5. Standard solutions and buffers for Western blot analyses.

Antibodies for Western Blot Analyses

Antibody	Clone	Application	Dilution	Company
RIG-I	Alme-1	TBST/5% MMP	1/1000	Enzo Life Science
MDA5	AT113	TBST/5% MMP	1/500	Enzo Life Science
LGP2	H-159	TBST/5% MMP	1/250	Santa Cruz Biotechnology
β-Actin	mAbcam	TBST	1/5000	Abcam

	8224			

Tab. 6. Primary antibodies for Western blot analyses.

Antibody	Clone	Application	Dilution	Company
Goat anti-rabbit pox	Polyclonal	TBST	1/7500	Dianova
Goat anti-mouse pox	Polyclonal	TBST	1/7500	Dianova

Tab. 7. Secondary antibodies for Western blot analyses.

Antibodies for FACS Analyses

Antibody	Clone	Format	Dilution	Company
Anti-CD3	SK7	FITC	1/100	Ebioscience
Anti-CD19	HIB19	FITC	1/100	Ebioscience
Anti-CD20	2H7	FITC	1/100	Ebioscience
Anti-CD56	MEM188	FITC	1/100	Ebioscience
Anti-CD141	AD5-14H12	(BDCA-3) PE	1/40	Miltenyi Biotec
Anti-CD123	6H6	PerCP-Cy5.5	1/40	Ebioscience
Anti-CD14	M5E2	PE/Cy7	1/200	BioLegend
Anti-CD11c	BU15	APC	1/100	Ebioscience
Anti-CD16	3G8	Alexa Fluor 700	1/100	BioLegend

Anti-CD1c	L161	APC/Cy7	1/100	BioLegend
Anti-CD86	IT2.2	Brilliant Violet 421	1/40	BioLegend
HLA-DR	L243	Brilliant Violet 605	1/40	BioLegend

Tab. 8. Antibodies for FACS analyses.

Methods

Isolation of PBMCs

To isolate PBMCs 20 ml of Biocoll separating solution were carefully overlayed on 25 ml of anticoagulated whole blood in a 50 ml Falcon tube for subsequent density gradient centrifugation as described schematically in Fig. 4. The tube was centrifuged at 2100 rpm for 20 min at RT. After centrifugation, blood cells were devided into different layers. The order of the layers is shown schematically in Fig. 4. Plasma was saved in 1.5 ml Eppendorf tubes and stored at minus 80° C for further analysis (not shown). PBMCs were carefully removed and transferred into a new 50 ml Falcon tube and subsequently washed by filling up the Falcon tube with precooled PBS followed by a centrifugation at 1500 rpm for 5 min at 4° C. The washing step was repeated twice. After discarding the respective PBS supernatants, the cell pellet was resuspended in 5ml of red blood cell lysis buffer and incubated for 5 minutes at RT. Thereafter, red blood cell lysis was stopped using 20 ml DC-Medium. The cells were centrifuged for 5 min at 1500 rpm and 4° C. After a white cell pellet was obtained, the supernatant was removed and the pellet was resuspended in 5 ml

of PBS and the number of cells was counted. At times of insufficient red blood cell lysis, lysis was repeated once more to entirely remove red blood cells. The cell number was determined using a Neubauer counting chamber.

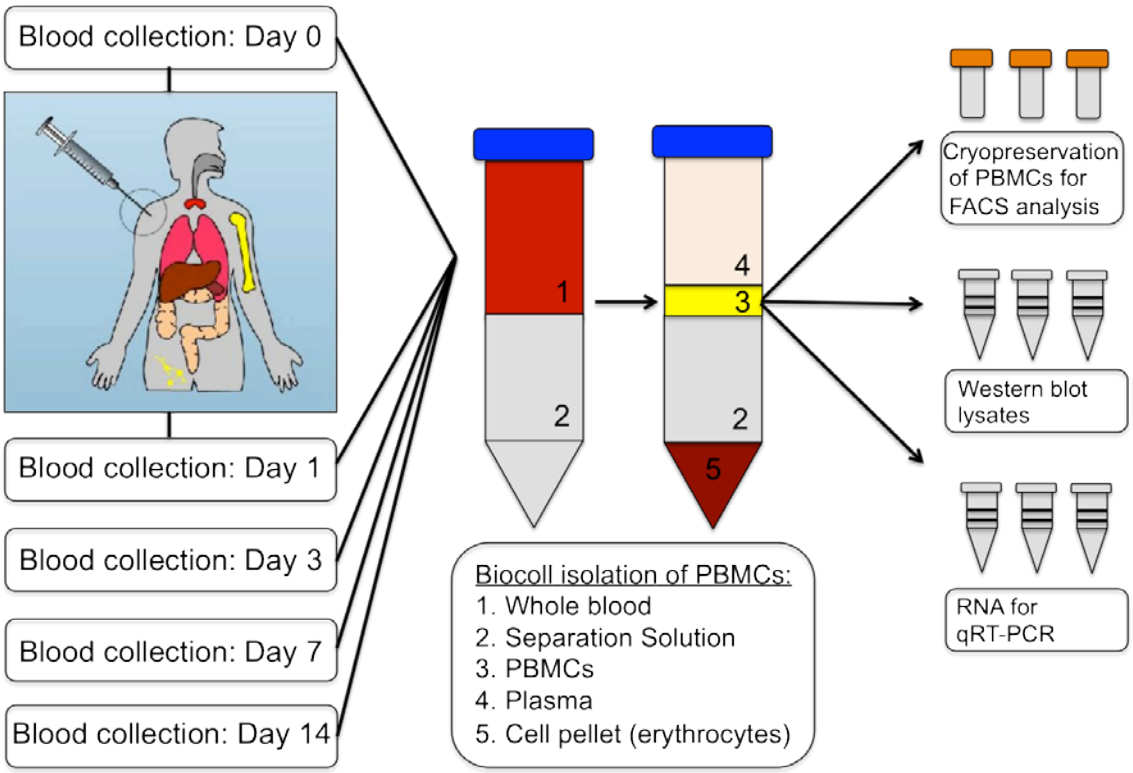

Fig. 4. PBMC preparation. Venous blood was drawn before vaccination on day 0. Thereafter, vaccination was performed. Additional blood collections were performed on days 1, 3, 7, and 14 as described in Methods. Blood samples were immediately transported to the laboratory at RT to perform Biocoll isolation of PBMCs within 120 minutes. Left 50 ml tube: Whole blood (1) was layered on top of the separation solution (2). Right 50ml tube: After centrifugation, the plasma layer (4) was taken off and PBMCs (3) were separated from the solution (2) and the erythrocyte pellet (5). PBMCs were divided into three samples: PBMCs for cryopreservation, Western blot lysates, and Trizol lysates for RNA isolation. The samples were stored as described in Methods.

Cryopreservation of PBMCs

To preserve isolated cells, cells were resuspended in freezing medium and aliquoted at $2x10^6$ cells/1 ml. Cryotubes were stored in special cryopreservation containers (Thermo Scientific) at -80° C for 48 hours and then transferred into liquid nitrogen for longterm storage.

Western Blot Lysate Preparation from PBMCs

PBMCs were resuspended in icecold PBS. $5x10^6$ cells were transferred into a 1.5 ml Eppendorf tube. Cells were spun down at 1500 rpm for 5 min at 4° C. The supernatant was discarded, the cell pellet then was resuspended in 80 µl of Western blot lysis buffer and incubated on ice for 15 min. The cells were centrifuged at 13000 rpm for 15 min at 4° C to spin down nuclei and the clear supernatant referred to as “whole cell lysate” was transferred into a new precooled 1.5 ml Eppendorf tube and stored at -20° C.

RNA Trizol Preservation

For qRT-PCR analyses $2x10^6$ PBMCs were transferred into an Eppendorf tube and centrifuged at 13 000 rpm for 15 min and the pellet was resuspended in 500 µl Trizol reagent. Trizol samples were stored at - 80° C until further use.

Western Blot Analysis

Protein concentrations were determined using the Bradford assay with bovine serum albumin as standard. The sample was diluted 1:1 with 2x Laemmli sample buffer and boiled at 95° C for 5 min. Whole cell lysated were separated using a 10 % SDS gel. Generally, 70 µg of protein in sample buffer was loaded onto each lane and proteins were separated in Bio-Rad Mini-Protean Cell at 100 V for 2 hours. Proteins were transferred to nitrocellulose membrane (GE Healthcare Life Sciences: Whatman Protran BA 85 (0,45 qm)) over night at 320 mA using a Wet/Tank blotting system. On day 2, nitrocellulose membranes were blocked in TBST + 5% skim milk powder for 2 hours and incubated

overnight using the primary antibody for RIG-I at the dilution given in table 6 and subsequently rinsed in TBST repeatedly (each rinse 10 minutes) for 90 minutes. For MDA-5 and LGP2 Western blots, nitrocellulose membranes which previously had been used for RIG-I detection, were stripped for 20 min using NaOH, membranes were blocked in TBST + 5% skim milk powder for 1 hour and subsequently incubated with antibodies as indicated in table 6. In stripped membranes, the dilution of the antibody against beta-actin was increased to 1/2000. Membranes were incubated with horseradish peroxidase-coupled secondary antibody diluted in TBST as shown in table 7 for 1 hr at RT at a concentration of 1/7500 for unstripped and at a concentration of 1/5000 for stripped membranes. Membranes were washed with TBST for 90 min. Protein bands were visualized using the Pierce Pico System as described by the manufacturer.

Semiquantitative Determination of Protein Bands

Semiquantitative determination of protein bands was performed after normalization using the beta-actin band as an internal standard using ImageJ 1.47v (Wayne Rasband National Institute of Health, USA http://imagej.nih.gov/ij). The intensity of each protein band was converted into a numerical value.

Analysis of Cells by Flow Cytometry

Distribution of immune cells among PBMCs was analyzed by fluorescence activated cell sorter (FACS) analyses using a Gallios Flow cytometer (Beckman Coulter) with the capacity to detect up to 10 different colors. Kaluza Flow

Analysis Software (Beckman Coulter) was used for data analyses. In brief, PBMCs were thawed in a 36° C water bath and transferred to a 50 ml Falcon tube. 4 ml FCS (4° C) were added dropwise and cells were centrifuged at 1500 rpm (4° C), the supernatant was removed, the cell pellet was washed 3 times in FACS buffer (5 ml each) to remove remaining DMSO. After the last wash, cells were suspended in 100 µl FACS buffer and transferred to 96 well plates. The plate was centrifuged at 1500 rpm (4° C) for 3 min and the supernatant was removed. 50 µl FACS buffer and human FC-Block (1/40) was added to each well and the plate was incubated for 15 min in the dark. After washing the cells with FACS buffer for 5 min, appropriate antibodies were added, the cells were incubated for 15 min on ice. After incubation the cells were centrifuged at 1500 rpm (4° C). 100 µl FACS buffer was added and cells were centrifuged at 1500 rpm (4° C). After this procedure was repeated 3 times, cells were diluted in 200 µl FACS buffer and transferred to FACS tubes. Just before analysis 5 µl of propidium iodide (1/20) was added to each FACS tube. 1 million events were acquired per sample on the FACS Gallios flow cytometer (Beckman Coulter).

	FL1	**FL2**	**FL3**	**FL4**	**FL5**	**FL6**	**FL7**	**FL8**	**FL9**	**FL10**
FL1		2,14	0,00	0,00	1,40	0,20	0,00	0,00	4,00	0,00
FL2	9,50		0,00	0,00	1,81	0,00	0,00	0,00	0,00	0,00
FL3	3,30	47,99		0,39	3,90	1,00	0,00	2,00	5,00	3,00
FL4	0,00	4,06	0,00		0,50	0,00	0,20	0,00	0,00	0,00
FL5	0,00	0,60	0,00	38,70		0,00	0,10	1,00	0,00	0,00
FL6	0,00	0,00	0,00	5,97	0,00		0,30	3,80	0,00	0,00
FL7	0,00	0,10	0,00	82,45	0,00	37,70		6,20	0,00	0,00
FL8	0,00	0,00	0,00	24,96	30,48	8,60	25,08		0,00	0,00

FL9	0,00	0,19	0,00	1,66	0,00	0,00	0,00	0,00		5,30
FL10	0,00	6,03	0,00	0,66	0,00	0,00	0,00	0,00	5,20	

Tab. 9. Flow cytometry compensation parameters used in this study.

qRT-PCR Analysis

RNA was isolated from PBMC using the TRIZOL reagent (Thermo Fisher Scientific) following the manufacturers instructions and reverse-transcribed to cDNA using SuperScript III reverse transcriptase. qRT-PCR analysis was performed using Taqman primer probe sets and Taqman Universal PCR Master mix (Applied Biosystems) according to the standard protocol by Applied Biosystems. Hypoxanthin-Phosphoribosyl-Transferase 1 was used as house keeping gene. Relative mRNA expression was quantified using the $2^{-\Delta\Delta CT}$ method. The steps using the Taqman prime probe sets generating qRT-PCR raw data was performed by Dr. rer. nat. Alexander Heiseke.

Statistics

Results are shown as mean values with standard error of the mean (SEM). Data was analysed using the repeated measures ANOVA with Bonferroni correction. Graph Pad Prism software version 5 was used for statistical analysis (http://www.graphpad.com/scientific-software/prism/).

3 RESULTS

Participating Volunteers

13 volunteers (7 females; 6 males; age range 23-32 years) (Tab. 10.) were enrolled in this study. Volunteers gave their written consent after they had been informed about the study protocol and the possible side effects of the blood draws. They received routine vaccination counseling at the Institute for Tropical Medicine, Ludwig-Maximilian-University and gave written consent to be vaccinated. The clinical study was approved by the Ethical Committee of the Technical University Munich according to international standards (project number: 5285/11). Blood was drawn by our collaborators at the Institute for Tropical Medicine of the Ludwig-Maximilians-University Munich and in the II. Medical Department, Klinikum rechts der Isar, Technical University Munich. All volunteers were free of any disease, allergy to egg protein or other constituents of the vaccination solution and immunosuppressive medication except volunteer M who informed us after the study that he was receiving Mesalazin for maintenance of remission of ulcerative colitis. None of the volunteers suffered any significant side effects.

Patient	**Sex**	**Age**	**Disease (Medication)**
A	Male	23	None
B	Female	29	None
C	Female	26	None

D	Male	26	None
E	Female	25	None
F	Female	26	None
G	Male	23	None
H	Female	23	None
I	Female	25	None
J	Male	28	None
K	Female	22	None
L	Male	32	None
M	Male	27	Ulcerative colitis (Mesalazin)

Tab. 10. Patient characteristics enrolled in this study.

Quantification of mRNA Expression of RIG-I and Selected Type I ISGs after Yellow Fever Vaccination

Total RNA was isolated from PBMC preparations and expression levels of mRNAs of RIG-I FL and of selected prototypic type I ISGs were determined by qRT-PCR: (DDX58; RIG-I), IRF7, ISG15, MX1, IP10, and CXCL10).

For RIG-I, the purpose to obtain qRT-PCR data during the course of the study was to examine whether there was regulation at the level of the mRNA and to correlate potential changes with those of the RIG-I proteins and with the type I IFN responses. The kinetics of mRNA expression in PBMCs showed constitutive expression of *RIG-I* before vaccination and a transient 2-3fold increase that became significant on day 3 ($p<0.05$) with an apparent peak at

day 7 ($p<0.01$) and a sharp return to baseline levels on day 14 (Fig 3). These data indicated that vaccination upregulates RIG-I mRNA (see below).

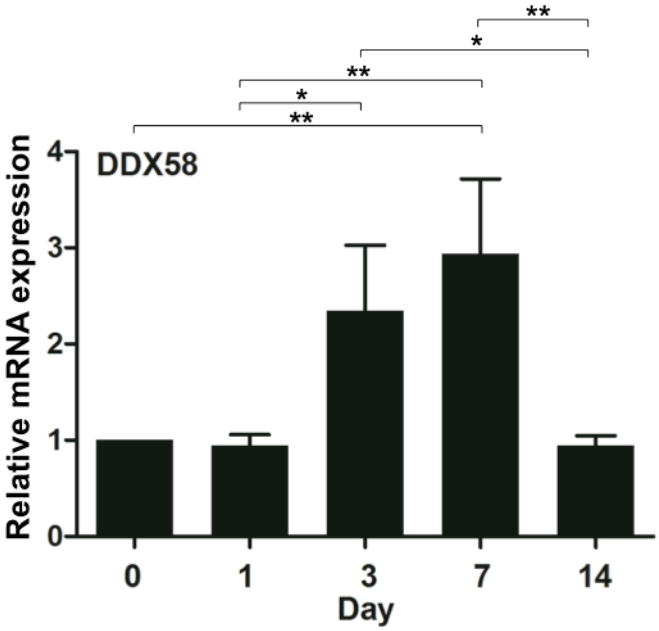

Fig. 5. Kinetics of DDX58 (RIG-I FL) relative mRNA expression. DDX58 relative mRNA levels were determined as described in Methods. Statistical significance was determined by ANOVA with Bonferroni correction. Mean values +/- SEM are shown. * $p < 0,05$; ** $p < 0,001$. n=13.

To further assess the type I IFN response to vaccination, we next analyzed several key type I ISGs in PBMCs. *IRF7* was chosen as a prototypic IFN-inducible gene (literature see discussion for further references). In our cohort of volunteers, *IRF7* mRNA was markedly induced on day 3 ($p<0.0001$) with a peak induction (4fold) on day 7 ($p<0.0001$), and a sharp decline to baseline levels on day 14 (Fig. 4). These data show that the kinetics of *IRF7* mRNA expression paralleled the expression of RIG-I mRNA.

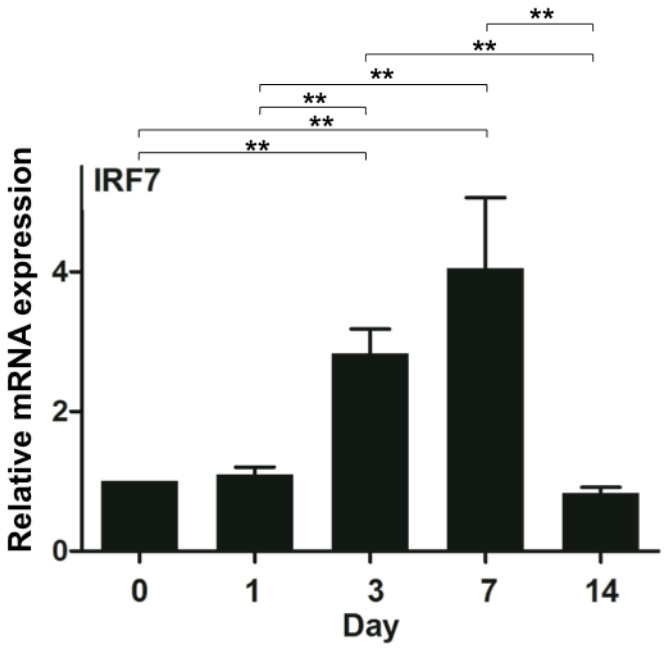

Fig. 6. Kinetics of IRF7 relative mRNA expression. IRF7 mRNA levels were determined as described in Methods. Statistical significance was determined by ANOVA with Bonferroni correction. Mean values +/- SEM are shown. ** p < 0,001. n=13.

ISG15 (ISG15 ubiquitin-like modifier) encodes an ubiquitin-like protein that is conjugated to intracellular proteins following activation by the type I IFNs. ISG15 mRNA was upregulated by a factor of approximately 7 on day 3 ($p<0.0001$) and by a factor of approximately 13 on day 7 ($p<0.0001$) to return to baseline levels by day 14 (Fig. 5). These data show that the kinetics of ISG15 mRNA induction after vaccination parallels those of RIG-I mRNA induction though the fold change is more pronounced than that of IRF7.

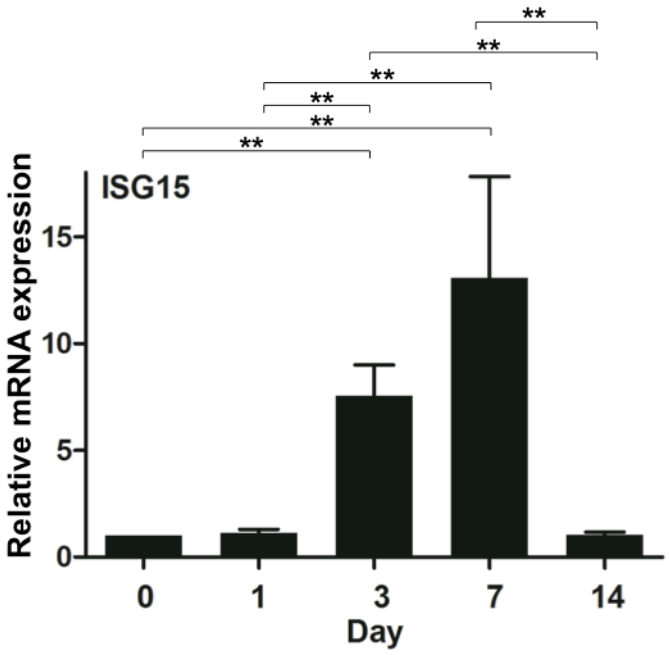

Fig. 7. Kinetics of ISG15 relative mRNA expression. ISG15 mRNA levels were determined as described in Methods. Statistical significance was determined by ANOVA with Bonferroni correction. Mean values +/- SEM are shown. ** p < 0,001. n=13.

MX1 (MX dynamin-like GTPase 1) encodes a guanosine triphosphate (GTP)-metabolizing protein that mediates antiviral responses. The encoded protein is induced by type I and type II IFNs and inhibits replication of RNA as well as a variety of DNA viruses (Gao et al., 2011). MX1 mRNA was induced on day 3 ($p<0.0001$) and day 7 ($p<0.0001$) and returned to baseline levels on day 14 (Fig. 6). The extent and kinetics of stimulation is similar to that of ISG15 indicating shared molecular mechanisms of induction.

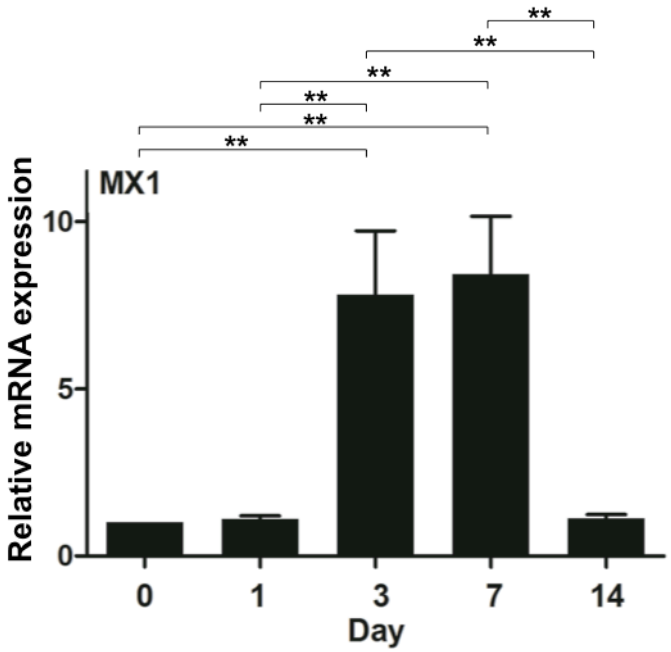

Fig. 8. Kinetics of MX1 relative mRNA expression. MX1 mRNA levels were determined as described in Methods. Statistical significance was determined by ANOVA with Bonferroni correction. Mean values +/- SEM are shown. ** p < 0,001. n=13.

CXCL10 (chemokine (C-X-C motif) ligand 10; IP-10) encodes an IFN inducible chemokine of the CXC family of chemokines. CXCL10 mRNA was markedly induced on day 3 ($p<0.001$) and 7 ($p< 0.001$) and returned to baseline levels on day 14 (Fig. 7).

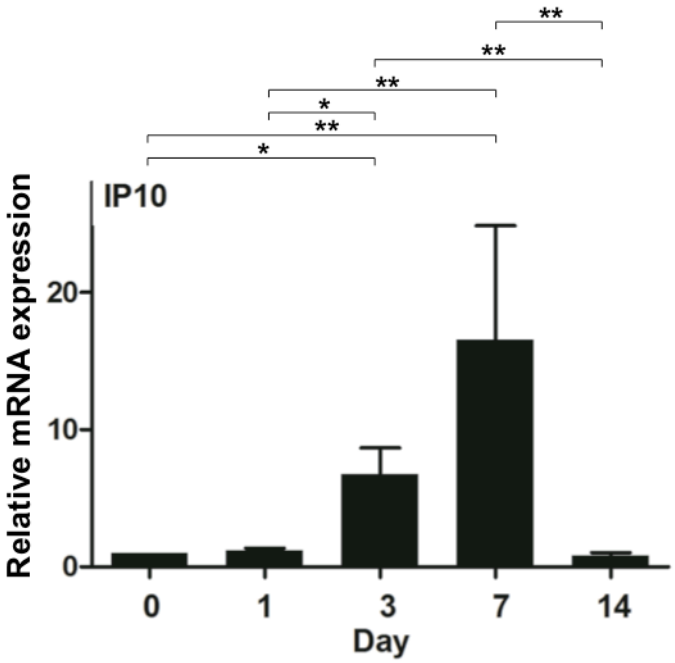

Fig. 9. Kinetics of IP10 relative mRNA expression. IP10 mRNA levels were determined as described in Methods. Statistical significance was determined by ANOVA with Bonferroni correction. Mean values +/- SEM are shown. * $p < 0,05$; ** $p < 0,001$. n=13.

When taken together, semiquantitative determination of mRNA expression of prototypic ISGs including RIG-I itself revealed robust induction between days 3-7 after vaccination. ISG mRNA expression returned to baseline levels on day 14 post vaccination. These data are consistent with published results obtained by large scale microarray analysis performed on whole blood in previous yellow fever vaccination studies (Querec et al., 2009; Gaucher et al., 2008).

Expression of RIG-I Protein Isoforms and other RLRs after Yellow Fever Vaccination

Western blot analyses were performed to detect expression of RIG-I isoform proteins in whole lysates of human PBMCs before and after vaccination within 14 days. Human PBMCs consist of lymphocytes (70-90%), monocytes (10-

30%), and DCs (1-2%) (see FACS analyses below). The expression of RIG-I isoforms *in vivo* and in humans is not known though it had previously been characterized *in vitro*. Representative results obtained from PBMCs of two volunteers (D and C) are shown using the monoclonal antibody Alme-1, which detects all three RIG-I variants (see Fig. 1 in introduction) due to its binding specificity for the helicase domain of RIG-I (Eisenächer, 2011) (Fig. 8). These analyses show a significant and marked expression of RIG-I FL protein before vaccination in all volunteers, two representative volunteers are shown in Fig. 8. Data demonstrate that RIG-I FL is constitutively expressed in PBMCs of healthy volunteers. Moreover, RIG-I FL protein was induced on day 7 and returned to the levels before vaccination on day 14 (Fig. 8). Although not visible in the Western blot before vaccination, RIG-I SV was detectable on days 3, 7, and 14 with prominent expression on day 7 (Fig. 8). However, the blots did not separate RIG-I FL and SV to a sufficient degree to allow semiquantitative statistical analyses using ImageJ software. RIG-I SF was not observed before vaccination although the densitometer picked up a weak signal. Importantly, however, all volunteers showed a strong increase of RIG-I SF on days 3, 7, and 14 (Fig. 8). Thus, RIG-I SF was induced much more vigorously (approximately by a factor of 12) when compared to RIG-I FL. These data reveal that while RIG-I FL is constitutively expressed in PBMCs of healthy naïve humans, both RIG-I SV and RIG-I SF are significantly induced early after vaccination with a peak at day 7. It is noteworthy that RIG-I SF remained elevated on day 14 when the other RIG-I isoforms had returned to prevaccination levels.

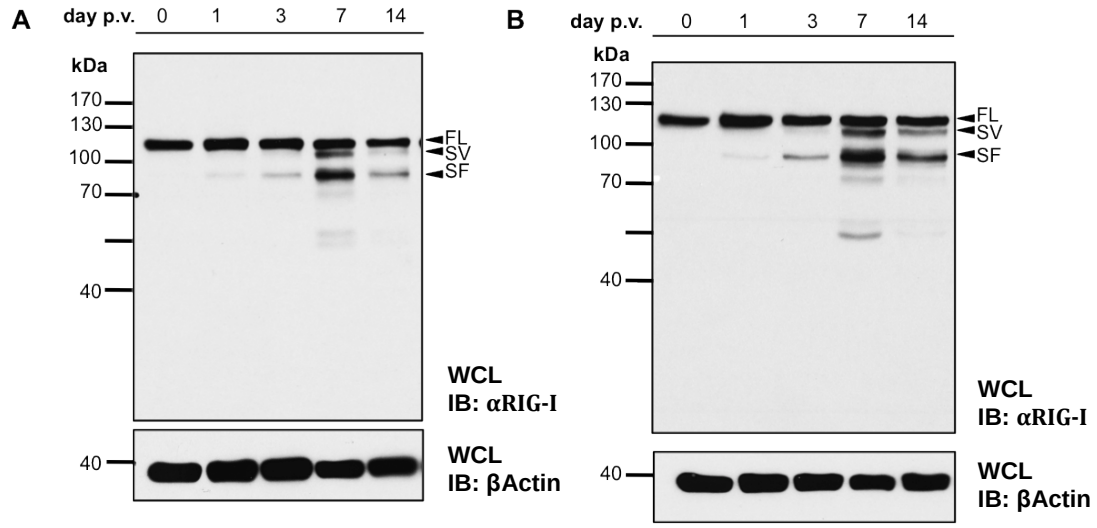

Fig. 10. Kinetics of RIG-I FL and RIG-I SF protein on PBMCs of representative volunteers. RIG-I FL, RIG-I SV, and RIG-I SF protein levels where determined by Western blot analyses as described in methods.

These data show that both RIG-I SV and RIG-I SF are undetectable before vaccination, upregulated on days 3,7, and 14, and that RIG-I SV and RIG-I SF are maintained at an elevated level on day 14.

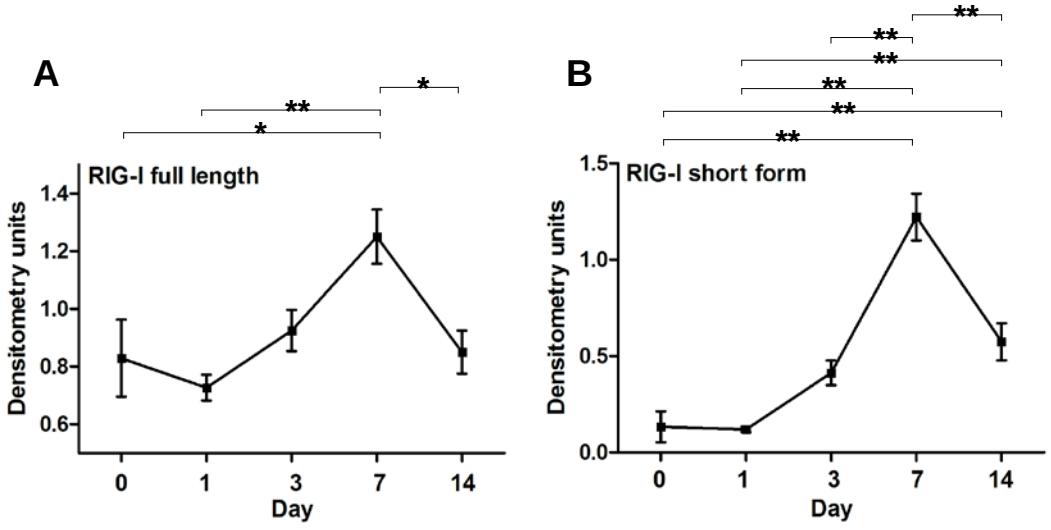

Fig. 11. Kinetics of RIG-I FL and RIG-I SF protein as determined by densitometry. (A) RIG-I FL protein and (B) RIG-I SF protein levels were determined by densitometry as described in methods (mean ± SEM). Statistical significance was determined by ANOVA with Bonferroni correction. * $p < 0,05$; ** $p < 0,001$. n=13.

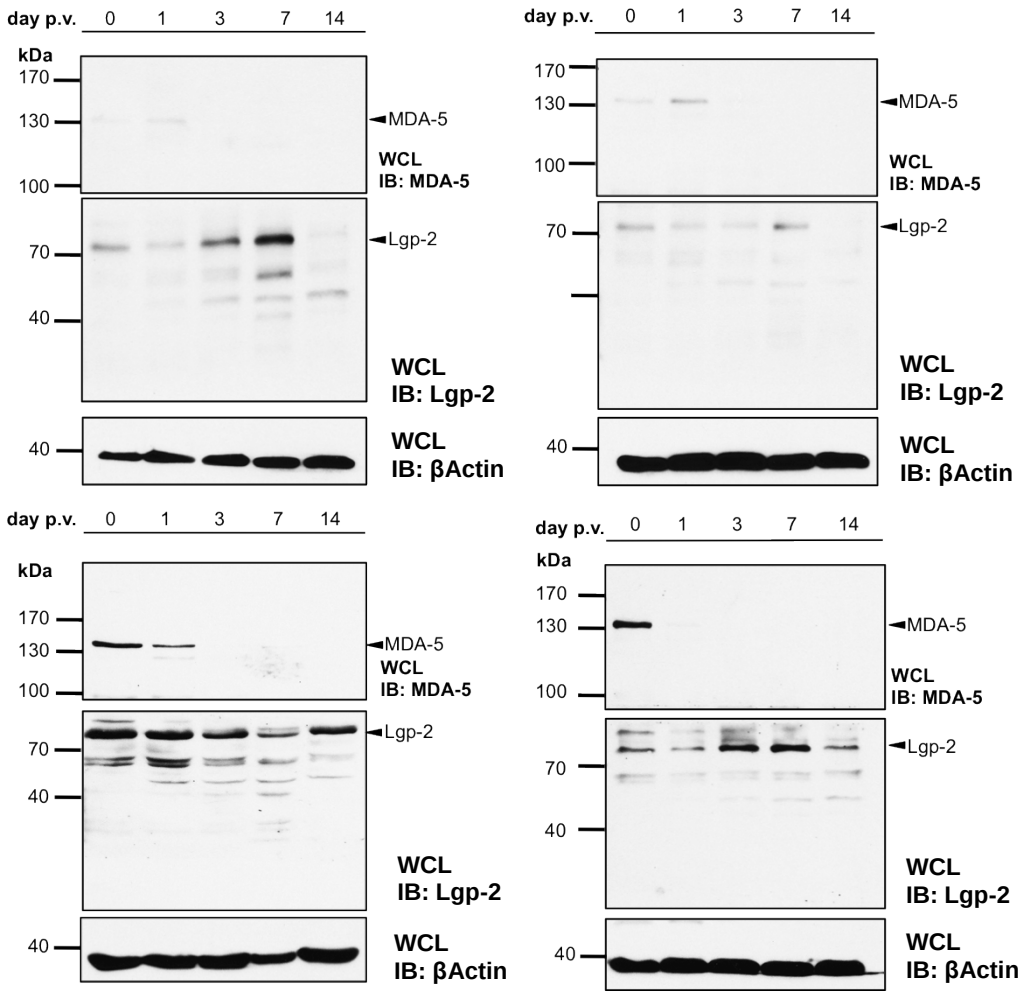

Fig. 12. Kinetics of MDA5 and LGP2 protein expression. MDA5 and LGP2 protein levels where determined by Western blot analyses as described in methods.

We next examined the two other members of the RLR family, i.e. MDA5 and LGP2. Several MDA5 antibodies were tested and the antibody dilution was optimized using lysate from MDA5-transfected cells (data not shown). Faint bands of MDA5 were detected in the samples of many donors showing that endogenous MDA5 is expressed at the detection limit of our assay. It was therefore not possible to quantify MDA5 expression by densitometry. However, MDA5 was detectable in all donors before vaccination indicating that MDA5 is expressed in PBMCs under steady state conditions. MDA5 seemed to be downregulated after vaccination. This was seen in all donors. Similar to RIG-I LGP2 was expressed before vaccination and was upregulated following kinetics

that resembled RIG-I, this has been seen in 10 of 12 volunteers. When taken together, MDA5 and LGP2 were differentially regulated following yellow fever vaccination with the LGP2 kinetics resembling RIG-I (Fig. 12).

Impact of Yellow Fever Vaccination on the Frequency of Monocyte and DC Subpopulations

Monocytes and DCs are equipped with TLRs and RLRs which can sense the yellow fever virus and they are responsible for the systemic innate cytokine response to the yellow fever vaccine. FACS analyses were performed on PBMC preparations to determine changes in relative numbers of monocytes and DC subpopulations and their activation state. The FACS gating strategy is shown schematically in Fig. 13.

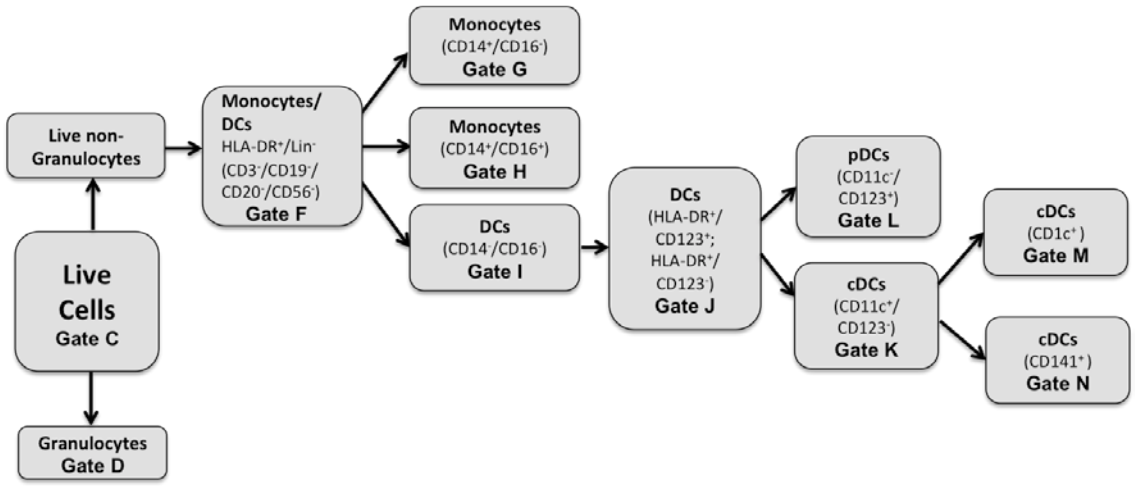

Fig. 13. Gating strategy to analyse the relative cell number of distinct immune cell subsets by FACS. Following isolation of PBMCs, frozen cells were thawed and the percentage of live cells was determined (gate C: live cells); non-granulocytes (gate D) were gated using CD16/side scatter. Subsequently, the relative sum of all monocytes/DCs was determined using HLA-DR/Lin ($CD3^-$; $CD19^-$; $CD20^-$; $CD56^-$; Gate F); $CD14^+$ monocytes were separated by their CD16 expression into classical and inflammatory monocytes (Gates G and H). DCs were gated by their double negativity for CD14 and CD16 (Gate I); all DCs (Gate J) were gated into pDCs ($CD11c^-/CD123^+$; Gate L) and all cDCs ($CD11c^+/CD123^-$; Gate K); and DC subtypes were gated into $CD1^+$ (Gate M) and $CD141^+$ DCs (Gate N).

PBMCs after gating out neutrophils (live non-granulocytes) were gated for monocytes and DCs (HLA-DR$^+$/Lin$^-$)(CD3$^-$/CD19$^-$/CD20$^-$/CD56$^-$). Two major types of monocytes (CD14$^+$/CD16$^-$ or classical monocytes and CD14$^+$/CD16$^+$ or inflammatory monocytes) and DCs (CD14$^-$/CD16$^-$) were separated; further gating was performed to delineate all DCs (HLA-DR$^+$/CD123$^+$; and HLA-DR$^+$/CD123$^-$), then for pDCs (CD11c$^-$/CD123$^+$) and cDCs (CD11c$^+$/CD123$^-$). Finally CD1c$^+$ (Breton et al., 2015) and CD141$^+$ subsets were distinguished within the cDC population (Fig. 11). The total monocyte population remained unchanged during the course of the study (data not shown). However, classical CD14$^+$/CD16$^-$ monocytes significantly decreased on day 7 (Fig. 15 and Fig. 19) whereas the proinflammatory CD14$^+$/CD16$^+$ monocyte subset increased on day 7 (Fig. 15 and Fig. 20). Moreover, there was no significant change in the total blood DC population. However, the number of pDCs (Reizis et al., 2011) decreased on day 14 (Fig. 17 and Fig 22). By contrast, CD1c$^+$ DCs showed an early increase which became significant on day 3 and day 7, and returned to baseline levels on day 14 (Fig. 18 and Fig. 23). Finally, CD141$^+$ DCs, were significantly down-regulated on day 7 and recovered on day 14 (Fig. 18 and Fig. 24).

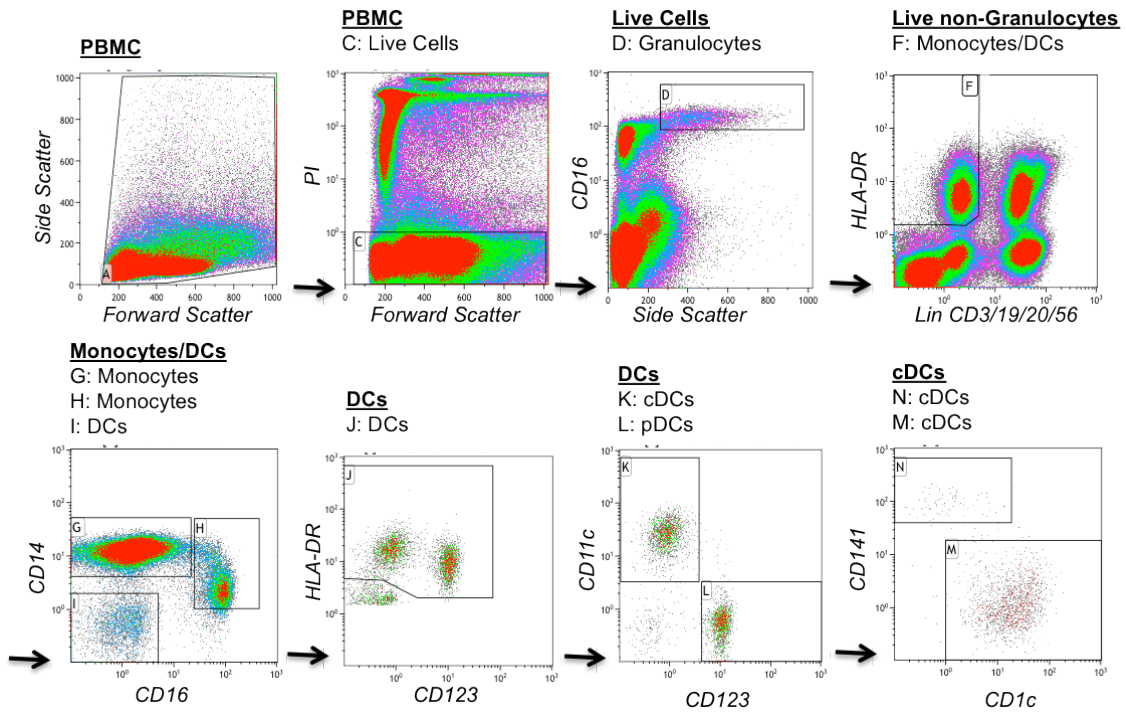

Fig. 14. Representative FACS dot blots of Patient B on day 0. FACS dot blots were acquired/generated as described in schematic Fig. 11. PBMCs were analyzed as described in Methods by gating as shown on the X- and Y-axes. Gates were designated C through M. For quantitative determination and statistics across all volunteers see below.

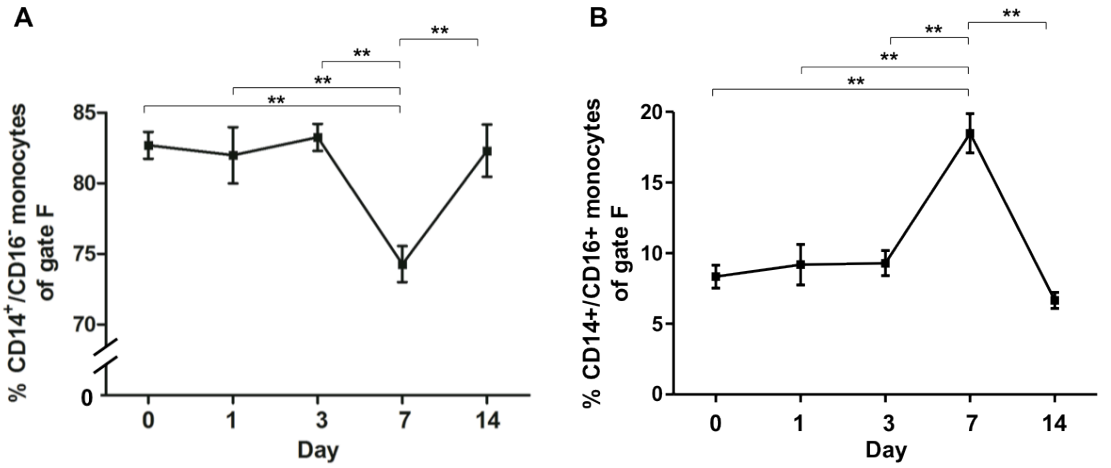

Fig. 15. Percentages of CD14+/CD16- and CD14+/CD16+ monocytes of gate F. A: Classical $CD14^+/CD16^-$ monocytes of gate F decrease on day 7. Inflammatory $CD14^+/CD16^+$ monocytes of gate F increase on day 7. ANOVA and subsequent Student´s t-test was performed as described in Methods. Mean values +/- SEM are shown. ** $p < 0{,}001$.

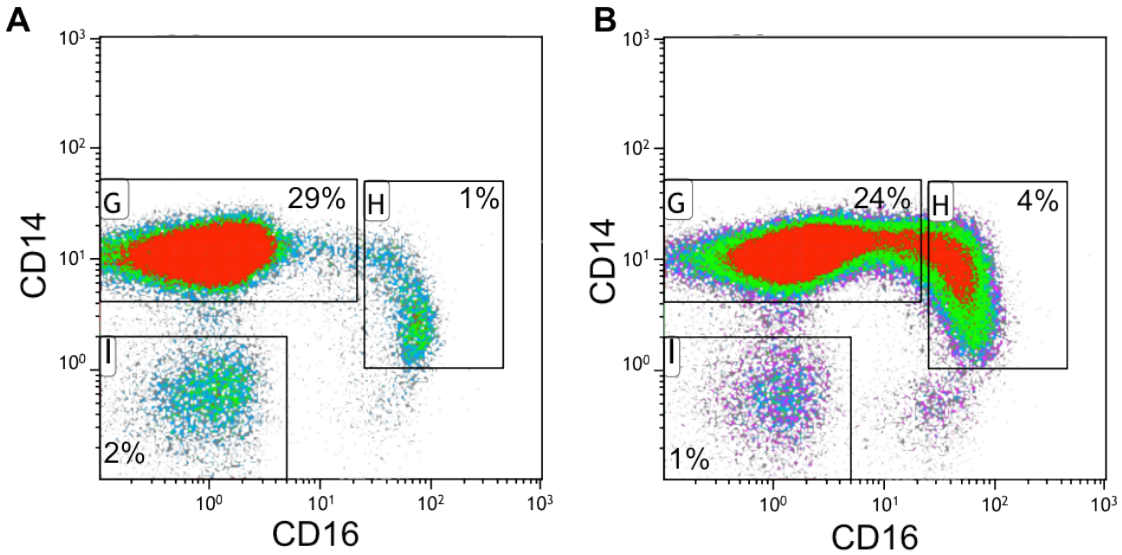

Fig. 16. Dot blot analyses of classical $CD14^+/CD16^-$ monocytes (gate G) and inflammatory $CD14^+/CD16^+$ monocytes (gate H) of a representative volunteer. A day 0; B day 7. Classical $CD14^+/CD16^-$ monocytes of gate F decrease on day 7.

These data show that in response to YF-17D vaccination the ratio of $CD14^+/CD16^+$ proinflammatory to classical $CD14^+/CD16^-$ monocytes increases at day 7 post vaccination in parallel with peak virus titers and the expression of ISGs. At the same time point, the ratio of $CD1c^+$ DCs to $CD141^+$ DCs increases.

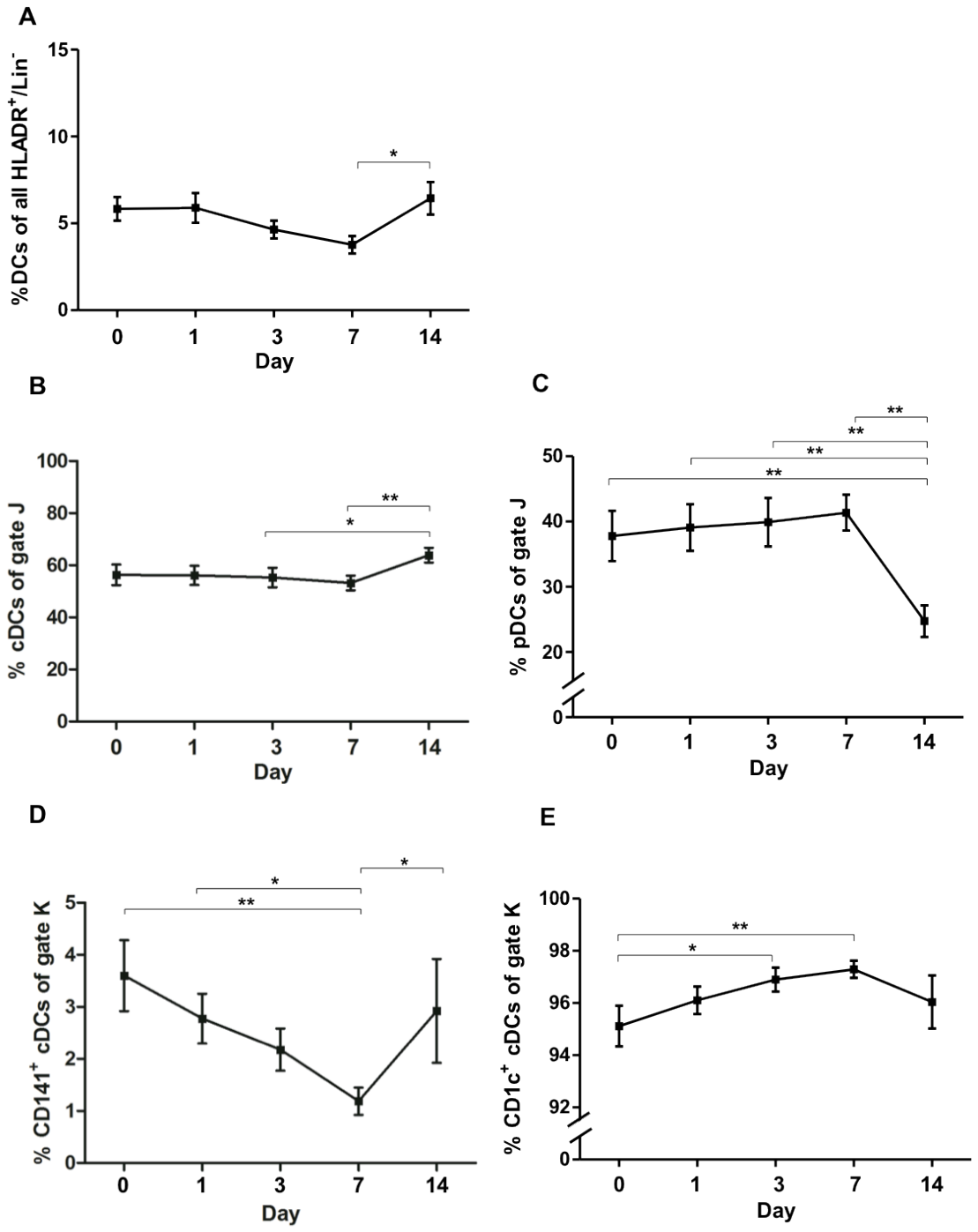

Fig. 17. Abundancy of DC subsets before and after vaccination.
A % DCs of HLA-DR$^+$/Lin$^-$; B % cDCs of gate J; C % pDCs of gate J; D % CD141$^+$ cDCs of gate K; E % CD1c$^+$ cDCs of gate K. Mean values +/- SEM are shown. * $p < 0,05$; ** $p < 0,001$. n=13.

Activation of Monocytes and DCs after Vaccination

We next examined the expression of HLA-DR and CD86 involved in antigen presentation and costimulation of T cells, respectively, on monocytes and DC

subtypes. Both $CD14^+/CD16^-$ and $CD14^+/CD16^+$ monocyte subsets showed significant upregulation of both HLA-DR and CD86 on day 7 when compared to the prevaccination time point (Fig. 18, Tab. 11). In addition, $CD141^+/CD1c^-$ cDCs showed upregulation of CD86 but not of HLA-DR whereas $CD141^+/CD1c^+$ cDCs showed upregulation of HLA-DR but not of CD86. In contrast, no change in either HLA-DR or CD86 was observed in pDCs (Tab. 11). These data provide evidence that both monocyte subsets and cDCs are activated by vaccination.

Immune Cell Subset	**HLA-DR** (MFI) **Day 0**	**HLA-DR** (MFI) **Day 7**	**p-value**	**CD86** (MFI) **Day 0**	**CD86** (MFI) **Day 7**	**p-value**
$CD14^+/CD16^-$ Monocytes	6.0 ± 0.4	7.9 ± 0.6	<0.01	2.5 ± 0.1	3.6 ± 0.1	<0.01
$CD14^+/CD1^+$ Monocytes	10.9 ± 0.8	15.9 ± 1.3	<0.01	3.4 ± 0.2	4.8 ± 0.3	<0.01
$CD141^+/CD1c^-$ cDCs	11.4 ± 1.1	9.6 ± 0.6	ns	1.0 ± 0.0	1.1 ± 0.0	<0.05
$CD141^-/CD1c^+$ cDCs	18.2 ± 1.1	14.7 ± 1.1	<0.01	1.3 ± 0.1	1.4 ± 0.1	ns
$CD11c^-$ $/CD123^+$ DCs (pDCs)	12.8 ± 1.5	12.3 ± 1.5	ns	1.2 ± 0.3	1.4 ± 0.3	ns

Tab. 11. FACS analyses of HLA-DR and CD86 on PBMC subsets. Percentages of HLA-DR or CD86 positive PBMC subsets were determined in respective gates on day 0 and day 7. MFI: Mean fluorescence intensity. Statistics were determined by ANOVA with Bonferroni correction. Mean values +/- SEM are shown. *<0,05; **<0,01. n=13.

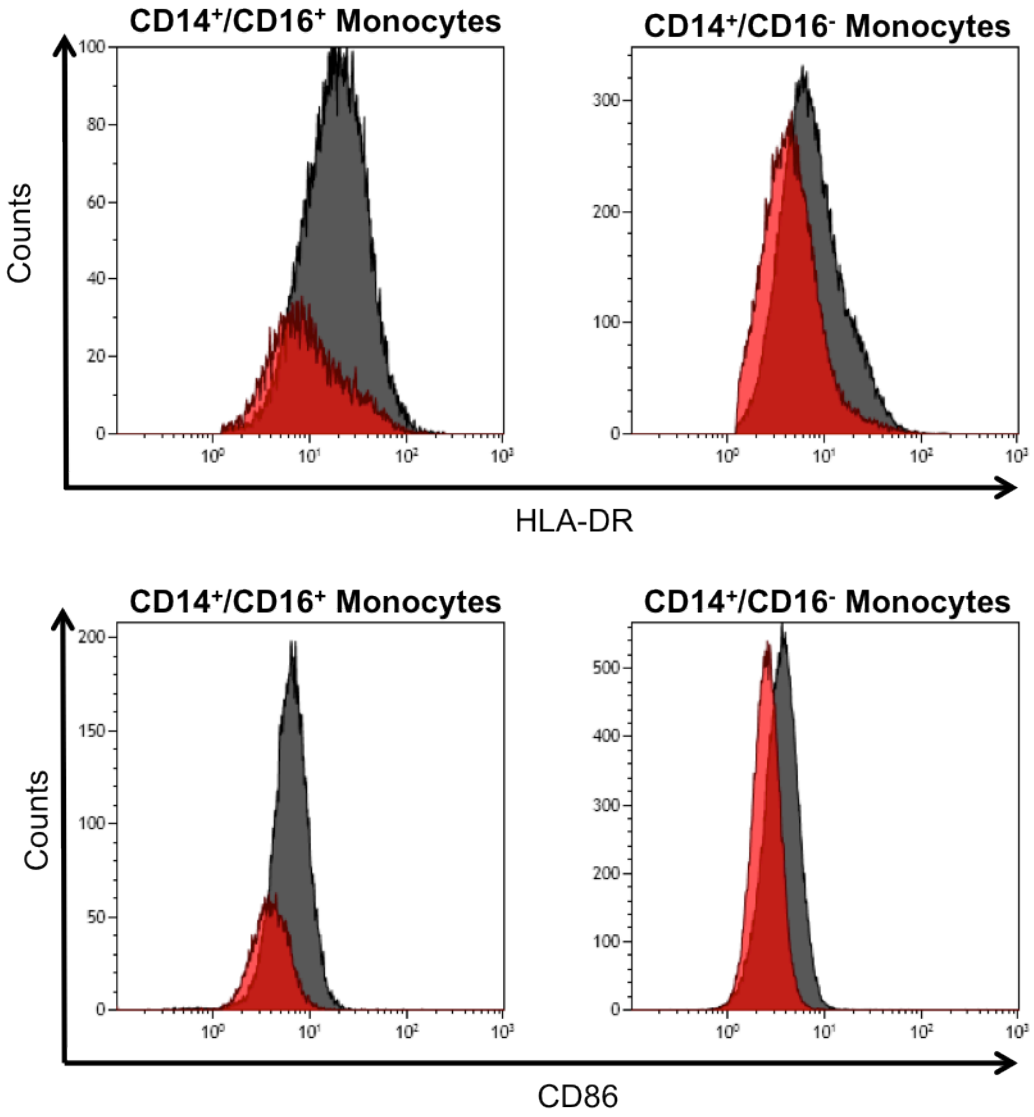

Fig. 18. FACS analyses of HLA-DR and CD86 positive cells in PBMC subsets on day 0 and day 7. FACS analyses on a representative volunteer were performed as described in Methods. Red, day 0; black, day 7. Statistics on all volunteers are reported in Table 11.

4 DISCUSSION

The body of data presented above can be summarized as follows: Immunization against yellow fever by YF-17D-204 triggers a profound response of the innate immune system in healthy human volunteers as evidenced by major alterations in PBMCs: Induction of RIG-I mRNA, induction of RIG-I FL, RIG-I SV, and RIG-I SF at the levels of the RIG-I protein isoforms, marked up-regulation of prototypic type 1 ISGs, and differential alterations in the number of PBMC subpopulations including relative down-regulation of classical $CD14^+/CD16^-$ monocytes concomitantly with up-regulation of inflammatory $CD14^+/CD16^+$ monocytes; up-regulation of $CD1c^+$ DCs at day 3 and 7; down-regulation of $CD141^+$ DCs at day 7, and down-regulation of pDCs at day 14. Moreover, marked and sustained up-regulation of RIG-I SF was observed. These results show for the first time that RIG-I SF, for which a negative regulatory function has been shown *in vitro*, is induced and maintained during viral infection *in vivo* in humans.

YF-17D Triggers Marked Upregulation of RIG-I SF

RIG-I SF protein is derived from RIG-I FL protein through proteolytic cleavage following RIG-I FL translation (unpublished data). As RIG-I SF is not expressed before vaccination, unlike RIG-I FL, these data reveal that RIG-I SF production is induced by the viral infection, most likely by type I IFNs as previously shown in vitro. Moreover, RIG-I SF remains elevated at day 14, i.e. the time point when all IFN-inducible gene mRNAs have returned to baseline levels. The sustained elevated level of RIG-I SF therefore strongly suggests that either the protease

that cleaves RIG-I SF from RIG-I FL is maintained at a high activity level at this time point or that the biological half life of RIG-I SF is quite long. Regardless of these unanswered questions, the elevated level of RIG-I SF at day 14 after vaccination supports the hypothesis that it plays a regulatory role after the initial induction of the innate immune response. Since protein analysis was done using lysates of whole PBMC, it cannot be excluded that RIG-I isoform expression as seen in Western blot analysis of PBMC lysates is influenced by changes in the composition of PBMC or recruitment of newly produced leukocytes from the bone marrow. To gain further insight into the expression of RIG-I and its isoforms in the various immune cell subsets, it will be necessary to isolate them by FACS cell sorting, then perform Western blot analyses of the isolated cells.

YF17D Vaccination Modulates MDA5 and LGP2 Expression in PBMC

Yellow fever vaccination affects not only RIG-I but also the two other RLR family members, i.e. MDA5 and LGP2. Unexpectedly, MDA5 in PBMC was found to be downregulated after vaccination. Subsequent analysis of MDA5 mRNA expression revealed that MDA5 was induced at the mRNA level with similar kinetic as other ISG (data not shown). It can be speculated therefore that translation of MDA5 mRNA is inhibited or that MDA5 protein is rapidly degraded in PBMC in response to YF17D vaccination. This speculation seems conceivable in view of reports that MDA5 filament mutations have been described to show that overstabilization of MDA5 protein can cause inflammatory diseases (del Toro Duany et al., 2015). This could be caused directly by the virus as a viral immune evasion mechanisms, as YF17D was reported to activate RLRs including MDA5. Alternatively, the reduction of MDA5

protein expression could be caused indirectly by cytokine stimulation possibly via targeting E3 ubiquitin ligases through indirectly affecting cytokine production by macrophage subsets (Goru et al., 2016). Further studies are required to investigate the regulation of MDA5 protein expression after viral infection in vitro and in vivo.

The observation that LGP2 protein is not constitutively expressed, but induced with similar kinetics as RIG-I confirms previous in vitro findings, which show that LGP2 is induced by type I interferon LGP2, which is signaling-inactive due to the lack of CARDs, was reported to act as a negative feedback regulator of the RIG-I pathway in vitro (Rothenfusser et al., 2005). On the contrary, studies using LGP2 knockout mice have shown that LGP2 may act upstream of RIG-I and MDA5 as an enhancer of the RLR signaling pathway (Satoh et al., 2010; Bruns et al., 2014). The role of LGP2 for the innate antiviral immune response and its regulation is not clear at the moment, but the prominent induction found in PBMC after infection with YF17D suggests that it participates in the immune response to this attenuated flavivirus.

ISGs are Triggered Early After Vaccination

IRF7 is a member of the IFN regulatory transcription factor (IRF) family, which has been shown to play a role in the transcriptional activation of virus-inducible cellular genes, including IFN-β chain genes. Interestingly, pDCs (see below) were unable to express type I IFN genes in a patient described in Ciancanelli et al. who suffered from heavy influenza virus load (Ciancanelli et al., 2015). Moreover, IRF7 plays important roles in many virus infections other than yellow fever and also in cancer biology (Honda et al., 2006; Dai et al., 2004; Zhu et al., 2002; Bidwell et al., 2012; Guiducci et al., 2008). In the present study, IRF7

mRNA was transiently up-regulated on days 3 and 7, then returned to baseline levels by a factor of up to 4fold indicating both positive and negative feedback regulatory mechanisms during the 14 day observation period. ISG15 encodes an ubiquitin-like protein that is conjugated to intracellular proteins downstream of activation by IFNα and IFNβ. Functions include chemotactic activity towards neutrophils and antiviral activity (Broering et al., 2010; Durfee et al., 2010; Durfee et al., 2010). Moreover, ISG15 protein is sometimes secreted (Skaug and Chen, 2010). MX1 encodes a guanosine triphosphate (GTP)-metabolizing protein that participates in the cellular antiviral response (Haller and Kochs, 2011; Verhelst et al., 2012; Gao et al., 2011). The encoded protein is induced by both type I and type II IFNs and antagonizes the replication process of several different RNA and DNA viruses (Gao et al., 2011). Similarly to IRF7 and ISG15, MX1 mRNA showed a transient response that amounted to an up to 8fold induction on days 3 and 7, respectively. CXCL10 (chemokine (C-X-C motif) ligand 10; alias IP-10) encodes a chemokine of the C-X-C family of chemokines. CXCL10 is a ligand for the receptor CXCR3 (Liu et al., 2011; Ichikawa et al., 2013; Berenguer et al., 2012). Binding of CXCL10 to CXCR3 results in multiple effects, including stimulation of monocytes, natural killer cells, and T cell migration (Deng et al., 2008). CXCL10 mRNA was markedly induced on days 3 and 7 with a peak stimulation of approximately 17-fold on day 7. When taken together, these prototypic ISGs showed marked up-regulation during the course of 7 days after vaccination and returned to baseline levels at day 14. Since peak virus loads are reached at day 7 and decrease thereafter, these data show that YF-D17 triggers a robust and well regulated IFN response.

Differential Regulation of Innate Immune Cell Subsets of PBMCs

$CD14^+$ monocytes make up a significant proportion of all live non-granulocytes. This major constituent of all nonlymphoid immune cells in the circulation consists of $CD14^+/CD16^-$ classical monocytes (Hofer et al., 2015), and $CD14^+/CD16^+$ inflammatory monocytes (Hofer et al., 2015). Within the $HLADR^+Lin^-/CD14^-/16^-$ fraction $CD141^+$ cDCs, $CD1c^+$ cDCs, and pDCs (Banchereau and Steinman, 1998; Dudziak et al., 2007; Fogg et al., 2006; Ginhoux et al., 2009; Liu, 2005; Liu et al., 2009; Bunin et al., 2015; Steinman, 2012) are found. Our data reveal differential regulation of the number of these innate immune cell subsets in the circulation in response to yellow fever vaccination: Each of these innate immune cell subsets are assumed to play a specific role in the course of immune system activation through the secretion of cytokines and the bridging of the innate immune system to the adaptive immune system carried out by B and T cells. Bridging of the innate and the adaptive immune system by monocytes/macrophages and DCs will result in activation and shaping of T cells to trigger a cellular adaptive immune response and in humoral immune protection by immunoglobulins directed against the yellow fever virus. Especially prominent was the increased frequency and activation of $CD14^+/CD16^+$ monocytes, which correlated with peak expression of ISGs after YF17D vaccination. This subset of monocytes, was reported to have proinflammatory function due to its capacity to produce higher amounts of TNF, IL-1, and IL-6 than conventional $CD14^+/CD16^-$ monocytes. Several studies have reported an expansion of this population during systemic inflammatory responses for example in sepsis patients, but also in response to viral infection (Williams et al., 2014; Heinbockel et al., 2015; Scherer et al., 2007; Mohanty et al., 2015; Kwissa et al., 2014).

In future studies each of these immune cell subsets should be isolated and its transcription response, i.e. their transcriptomes, should be determined within the time course of at least 14 days. Such data will deepen our understanding of the roles of each innate immune cell subset in viral infection. Moreover, it would be of interest to perform Western blot analyses of the isolated immune cell subpopulations to more specifically understand the cells in which both RIG-I FL protein and its proteolytic cleavage product, i.e. RIG-I SF, are induced.

YF-17D vaccination is highly effective to protect from yellow fever. This life virus vaccination is a suitable research tool to study the immune response in humans and findings obtained from these studies may be applicable to other virus infections including the human immunodeficiency virus (Trumpfheller et al., 2012). Besides the central role of type I IFN responses in infection, the roles of type I IFN responses in cancer biology, the pathogenesis of autoimmune diseases, and chronic inflammatory diseases also deserve attention (Kato and Fujita, 2015; Goldmann et al., 2016; Zitvogel et al., 2015; van Kempen et al., 2015). Thus, the current data on RIG-I SF may have a scope that goes beyond the pathophysiology of yellow fever pathology.

RIG-I SF May be a New Therapeutic Target to Inhibit or Enhance Type I IFN Responses in a Growing Number of Disease Conditions

Since the early 70s, type I IFN-related research became aware of the possibility that a series of human diseases may be due to aberrant type I IFN responses, referred to as *interferonopathies* (Crow and Manel, 2015). Since then, a growing number of *rare genetically determined disease conditions* in humans have been

categorized as interferonopathies including the *Aicardi-Goutières syndrome*, *Chilblain Lupus*, *Systemic Lupus Erythematodes*, *Idiopathic Intracranial Calcification, Singleton-Merten syndrome*, and others. Elucidation of these rare interferonopathies and their clinical manifestations have allowed to develop new concepts of the role of type-I IFNs in disease conditions as varied as virus infection, autoimmunity, and cancer. The concept has been that dysregulated, i.e. overshooting, type I IFN responses have detrimental effects largely on the nervous system, skin, and in systemic autoinflammation (Crow and Manel, 2015). It became apparent that while activation of RLRs by PAMPs induces a potent type I IFN response to suppress viral replication, it also can lead to tissue destruction. Thus, the immune system must walk a fine line between type I IFN-dependent antiviral activities and tissue destruction to maintain tissue homeostasis (Lee-Kirsch et al., 2015). In the interferonopathies, the immune system is inefficient to distinguish between self and nonself due to an overshooting IFN response. Clearly, the balance between stimulation and inhibition of ribonucleic acid-induced alterations in the immune system must be maintained in a well regulated way in order to eliminate the infectious agent without tissue injury. RIG-I SF may be an important endogenous negative feedback regulator in the maintenance of tissue homeostasis during yellow fever vaccination, yellow fever infection, and possibly other antiviral responses including Ebola and Marbus virus infections that all involve RIG-I as a major virus sensor (Messaoudi, I et al. 2015). In view of the discovery of RIG-I SF in this laboratory and the current results of its regulation and sustained expression *in vivo* after YF-D17 vaccination *in vivo* in humans, it will be of major interest to determine whether there is dysregulation of RIG-I SF in the established genetically determined diseases that have been recognized as *bona fide*

interferonopathies. In particular, genetic mutations have already been identified for RIG-I itself or another functionally important endogenous mediator of the IFN response, i.e. ISG15 (Crow and Manel, 2015; Kato and Fujita, 2015). It would be interesting to investigate, if interferonopathies that involve RIG-I are also associated with a dysregulation of RIG-I SF as this RIG-I isoform is a direct proteolytic cleavage product of RIG-I FL. In this regard, the early hypothesis and vision by Ion Gresser 35 years ago, that interferonopathies may result from an overshooting IFN responses, i.e. an IFN response at the wrong time, or during an extended time window (Gresser et al., 1980), holds significance until today. Obviously, any immunotherapy developed in experimental studies or in experimental models of interferon actions requires careful scrutiny before application in humans can be considered. The first step would be to test overexpression of RIG-I SF in preclinical disease models in which RIG-I-dependent type I IFNs are harmful to the host.

However, in other diseases, a type I IFN response may be needed such as in acute viral infections. It is well recognized that for example the Ebola and Marburg viruses both of which are sensed by RIG-I evade the innate immune system by their ability to produce proteins that directly inhibit the RIG-I signaling pathway and often the IFN induction and IFNα receptor (IFNAR1; IFNAR2) pathways which results in a failure of the innate immune system to prevent virus replication (Messaoudi et al., 2015). Thus, patients with Ebola virus and Marburg virus infection suffer from a lack of type I IFN responses (Messaoudi et al., 2015) resulting in lethal clinical outcomes in many patients. Moreover, although more work is required, the human cytomegalovirus (member of the herpes virus family) has multiple effects on the RIG-I degradation due to virus-

encoded inhibitors impairing caspase-dependent RIG-I degradation (Amsler et al., 2013)). Other immune evasion mechanisms involve direct effects on IFNARs and inhibition of ISG transcription (Sedger, 2013; Parks and Alexander-Miller, 2013). Under circumstances of reduced IFN responses, it may be beneficial to inhibit the endogenous negative feedback regulator of RIG-I signaling, i.e. RIG-I SF. These issues are complicated as IFN responses - in order to be effective – must occur during distinct time windows of virus infections. Clearly, further work on RIG-I SF in experimental models is needed.

Outlook: Both overshooting and suppression of the type I IFN response result in potentially lethal consequences for the host: i) A failure to eliminate lethal virus infections by viruses that evade the immune system will result in an overwhelming virus load because the immune system is prevented from mounting an appropriate IFN response; ii) conversely, in disease conditions that are characterized by an overshooting IFN response as exemplified by the interferonopathies, the virus load will be eliminated effectively; however, the IFN response will lead to tissue injury. In both circumstances, the balance between IFN responses and protection of the host tissue, cannot be maintained. It is apparent, that both the stimulatory arms and the negative control mechanisms to limit the IFN response, are potential therapeutic targets. The discovery of RIG-I SF and its regulation in vivo as exemplified in the innate immune response after YF-D17 vaccination in humans have therapeutic potential in disease conditions in which the RIG-I sensor plays a crucial role.

REFERENCES

Altfeld, M., and Gale Jr, M. (2015). Innate immunity against HIV-1 infection. Nature immunology *16*, 554-562.

Amsler, L., Verweij, M.C., and DeFilippis, V.R. (2013). The tiers and dimensions of evasion of the type I interferon response by human cytomegalovirus. Journal of molecular biology *425*, 4857-4871.

Banchereau, J., and Steinman, R.M. (1998). Dendritic cells and the control of immunity. Nature *392*, 245-252.

Barbalat, R., Ewald, S.E., Mouchess, M.L., and Barton, G.M. (2011). Nucleic acid recognition by the innate immune system. Annual review of immunology *29*, 185-214.

Beignon, A.-S., Skoberne, M., and Bhardwaj, N. (2003). Type I interferons promote cross-priming: more functions for old cytokines. Nature immunology *4*, 939-941.

Belgnaoui, S.M., Paz, S., and Hiscott, J. (2011). Orchestrating the interferon antiviral response through the mitochondrial antiviral signaling (MAVS) adapter. Current opinion in immunology *23*, 564-572.

Berenguer, J., Fernandez-Rodríguez, A., Jimenez-Sousa, M.A., Cosín, J., Zarate, P., Micheloud, D., López, J.C., Miralles, P., Catalán, P., and Resino, S. (2012). High plasma CXCL10 levels are associated with HCV-genotype 1, and higher insulin resistance, fibrosis, and HIV viral load in HIV/HCV coinfected patients. Cytokine *57*, 25-29.

Bidwell, B.N., Slaney, C.Y., Withana, N.P., Forster, S., Cao, Y., Loi, S., Andrews, D., Mikeska, T., Mangan, N.E., and Samarajiwa, S.A. (2012). Silencing of Irf7 pathways in breast cancer cells promotes bone metastasis through immune escape. Nature medicine *18*, 1224-1231.

Breton, G., Lee, J., Zhou, Y.J., Schreiber, J.J., Keler, T., Puhr, S., Anandasabapathy, N., Schlesinger, S., Caskey, M., and Liu, K. (2015). Circulating precursors of human CD1c+ and CD141+ dendritic cells. The Journal of experimental medicine *212*, 401-413.

Breugelmans, J., Lewis, R., Agbenu, E., Veit, O., Jackson, D., Domingo, C., Böthe, M., Perea, W., Niedrig, M., and Gessner, B. (2013). Adverse events following yellow fever preventive vaccination campaigns in eight African countries from 2007 to 2010. Vaccine *31*, 1819-1829.

Broering, R., Zhang, X., Kottilil, S., Trippler, M., Jiang, M., Lu, M., Gerken, G., and Schlaak, J.F. (2010). The interferon stimulated gene 15 functions as a proviral factor for the hepatitis C virus and as a regulator of the IFN response. Gut *59*, 1111-1119.

Browning, J.L. (2006). B cells move to centre stage: novel opportunities for autoimmune disease treatment. Nature Reviews Drug Discovery *5*, 564-576.

Brubaker, S.W., Bonham, K.S., Zanoni, I., and Kagan, J.C. (2015). Innate immune pattern recognition: a cell biological perspective. Annual review of immunology *33*, 257-290.

Bruns, A.M., Leser, G.P., Lamb, R.A., and Horvath, C.M. (2014). The innate immune sensor LGP2 activates antiviral signaling by regulating MDA5-RNA interaction and filament assembly. Molecular cell *55*, 771-781.

Bunin, A., Sisirak, V., Ghosh, H.S., Grajkowska, L.T., Hou, Z.E., Miron, M., Yang, C., Ceribelli, M., Uetani, N., and Chaperot, L. (2015). Protein Tyrosine Phosphatase PTPRS Is an Inhibitory Receptor on Human and Murine Plasmacytoid Dendritic Cells. Immunity *43*, 277-288.
Cella, M., Facchetti, F., Lanzavecchia, A., and Colonna, M. (2000). Plasmacytoid dendritic cells activated by influenza virus and CD40L drive a potent TH1 polarization. Nature immunology *1*, 305-310.
Chan, Y.K., and Gack, M.U. (2015a). RIG-I Works Double Duty. Cell host & microbe *17*, 285-287.
Chan, Y.K., and Gack, M.U. (2015b). RIG-I-like receptor regulation in virus infection and immunity. Current opinion in virology *12*, 7-14.
Chiang, J.J., Davis, M.E., and Gack, M.U. (2014). Regulation of RIG-I-like receptor signaling by host and viral proteins. Cytokine & growth factor reviews *25*, 491-505.
Ciancanelli, M.J., Huang, S.X., Luthra, P., Garner, H., Itan, Y., Volpi, S., Lafaille, F.G., Trouillet, C., Schmolke, M., and Albrecht, R.A. (2015). Life-threatening influenza and impaired interferon amplification in human IRF7 deficiency. Science *348*, 448-453.
Crow, Y.J., and Manel, N. (2015). Aicardi-Goutieres syndrome and the type I interferonopathies. Nature Reviews Immunology *15*, 429-440.
Dai, J., Megjugorac, N.J., Amrute, S.B., and Fitzgerald-Bocarsly, P. (2004). Regulation of IFN regulatory factor-7 and IFN-α production by enveloped virus and lipopolysaccharide in human plasmacytoid dendritic cells. The Journal of Immunology *173*, 1535-1548.
del Toro Duany, Y., Wu, B., and Hur, S. (2015). MDA5—filament, dynamics and disease. Current opinion in virology *12*, 20-25.
Deng, G., Zhou, G., Zhang, R., Zhai, Y., Zhao, W., Yan, Z., Deng, C., Yuan, X., Xu, B., and Dong, X. (2008). Regulatory polymorphisms in the promoter of CXCL10 gene and disease progression in male hepatitis B virus carriers. Gastroenterology *134*, 716-726. e712.
Dudziak, D., Kamphorst, A.O., Heidkamp, G.F., Buchholz, V.R., Trumpfheller, C., Yamazaki, S., Cheong, C., Liu, K., Lee, H.-W., and Park, C.G. (2007). Differential antigen processing by dendritic cell subsets in vivo. Science *315*, 107-111.
Durfee, L.A., Lyon, N., Seo, K., and Huibregtse, J.M. (2010). The ISG15 conjugation system broadly targets newly synthesized proteins: implications for the antiviral function of ISG15. Molecular cell *38*, 722-732.
Eisenächer, K. (2011). Functional analysis of cytosolic sensors of viral nucleic acids and their role for innate antiviral immune defense (Technische Universität München).
Eisenächer, K., and Krug, A. (2012). Regulation of RLR-mediated innate immune signaling–it is all about keeping the balance. European journal of cell biology *91*, 36-47.
Fogg, D.K., Sibon, C., Miled, C., Jung, S., Aucouturier, P., Littman, D.R., Cumano, A., and Geissmann, F. (2006). A clonogenic bone marrow progenitor specific for macrophages and dendritic cells. Science *311*, 83-87.
Gack, M.U., Kirchhofer, A., Shin, Y.C., Inn, K.-S., Liang, C., Cui, S., Myong, S., Ha, T., Hopfner, K.-P., and Jung, J.U. (2008). Roles of RIG-I N-terminal tandem CARD and splice variant in TRIM25-mediated antiviral signal transduction. Proceedings of the National Academy of Sciences *105*, 16743-16748.

Gack, M.U., Nistal-Villán, E., Inn, K.-S., García-Sastre, A., and Jung, J.U. (2010). Phosphorylation-mediated negative regulation of RIG-I antiviral activity. Journal of virology *84*, 3220-3229.
Gao, S., von der Malsburg, A., Dick, A., Faelber, K., Schröder, G.F., Haller, O., Kochs, G., and Daumke, O. (2011). Structure of myxovirus resistance protein a reveals intra-and intermolecular domain interactions required for the antiviral function. Immunity *35*, 514-525.
Gaucher, D., Therrien, R., Kettaf, N., Angermann, B.R., Boucher, G., Filali-Mouhim, A., Moser, J.M., Mehta, R.S., Drake, D.R., and Castro, E. (2008). Yellow fever vaccine induces integrated multilineage and polyfunctional immune responses. The Journal of experimental medicine *205*, 3119-3131.
Geginat, J., Sallusto, F., and Lanzavecchia, A. (2001). Cytokine-driven proliferation and differentiation of human naive, central memory, and effector memory CD4+ T cells. The Journal of experimental medicine *194*, 1711-1720.
Geissmann, F., Gordon, S., Hume, D.A., Mowat, A.M., and Randolph, G.J. (2010). Unravelling mononuclear phagocyte heterogeneity. Nature Reviews Immunology *10*, 453-460.
Ginhoux, F., Liu, K., Helft, J., Bogunovic, M., Greter, M., Hashimoto, D., Price, J., Yin, N., Bromberg, J., and Lira, S.A. (2009). The origin and development of nonlymphoid tissue CD103+ DCs. The Journal of experimental medicine *206*, 3115-3130.
Goldmann, T., Blank, T., and Prinz, M. (2016). Fine-tuning of type I IFN-signaling in microglia—implications for homeostasis, CNS autoimmunity and interferonopathies. Current opinion in neurobiology *36*, 38-42.
Gordon, S., and Taylor, P.R. (2005). Monocyte and macrophage heterogeneity. Nature Reviews Immunology *5*, 953-964.
Goru, S.K., Pandey, A., and Gaikwad, A.B. (2016). E3 ubiquitin ligases as novel targets for inflammatory diseases. Pharmacological Research *106*, 1-9.
Goubau, D., Deddouche, S., and e Sousa, C.R. (2013). Cytosolic sensing of viruses. Immunity *38*, 855-869.
Gresser, I., Morel- Maroger, L., Rivière, Y., Guillon, J.C., Tovey, M.G., Woodrow, D., Sloper, J.C., and Moss, J. (1980). INTERFERON- INDUCED DISEASE IN MICE AND RATS*. Annals of the New York Academy of Sciences *350*, 12-20.
Guiducci, C., Ghirelli, C., Marloie-Provost, M.-A., Matray, T., Coffman, R.L., Liu, Y.-J., Barrat, F.J., and Soumelis, V. (2008). PI3K is critical for the nuclear translocation of IRF-7 and type I IFN production by human plasmacytoid predendritic cells in response to TLR activation. The Journal of experimental medicine *205*, 315-322.
Guilliams, M., Ginhoux, F., Jakubzick, C., Naik, S.H., Onai, N., Schraml, B.U., Segura, E., Tussiwand, R., and Yona, S. (2014). Dendritic cells, monocytes and macrophages: a unified nomenclature based on ontogeny. Nature reviews Immunology *14*, 571.
Haller, O., and Kochs, G. (2011). Human MxA protein: an interferon-induced dynamin-like GTPase with broad antiviral activity. Journal of Interferon & Cytokine Research *31*, 79-87.
Heinbockel, L., Marwitz, S., Varela, S.B., Ferrer-Espada, R., Reiling, N., Goldmann, T., Gutsmann, T., Mier, W., Schürholz, T., and Drömann, D. (2015). Therapeutical Administration of Peptide Pep19-2.5 and Ibuprofen Reduces Inflammation and Prevents Lethal Sepsis. PloS one *10*, e0133291.

Hofer, T.P., Zawada, A.M., Frankenberger, M., Skokann, K., Satzl, A.A., Gesierich, W., Schuberth, M., Levin, J., Danek, A., and Rotter, B. (2015). Characterization of subsets of the CD16-positive monocytes: impact of granulomatous inflammation and M-CSF-receptor mutation. Blood, blood-2015-2006-651331.

Honda, K., Takaoka, A., and Taniguchi, T. (2006). Type I inteferon gene induction by the interferon regulatory factor family of transcription factors. Immunity *25*, 349-360.

Hornung, V., Ellegast, J., Kim, S., Brzózka, K., Jung, A., Kato, H., Poeck, H., Akira, S., Conzelmann, K.-K., and Schlee, M. (2006). 5'-Triphosphate RNA is the ligand for RIG-I. Science *314*, 994-997.

Ichikawa, A., Kuba, K., Morita, M., Chida, S., Tezuka, H., Hara, H., Sasaki, T., Ohteki, T., Ranieri, V.M., and dos Santos, C.C. (2013). CXCL10-CXCR3 enhances the development of neutrophil-mediated fulminant lung injury of viral and nonviral origin. American journal of respiratory and critical care medicine *187*, 65-77.

Iwasaki, A., and Pillai, P.S. (2014). Innate immunity to influenza virus infection. Nature Reviews Immunology *14*, 315-328.

Kapsenberg, M.L. (2003). Dendritic-cell control of pathogen-driven T-cell polarization. Nature Reviews Immunology *3*, 984-993.

Kato, H., and Fujita, T. (2015). RIG-I-like receptors and autoimmune diseases. Current opinion in immunology *37*, 40-45.

Kell, A.M., and Gale, M. (2015). RIG-I in RNA virus recognition. Virology *479*, 110-121.

Kurosaki, T., Kometani, K., and Ise, W. (2015). Memory B cells. Nature Reviews Immunology.

Kwissa, M., Nakaya, H.I., Onlamoon, N., Wrammert, J., Villinger, F., Perng, G.C., Yoksan, S., Pattanapanyasat, K., Chokephaibulkit, K., and Ahmed, R. (2014). Dengue virus infection induces expansion of a CD14+ CD16+ monocyte population that stimulates plasmablast differentiation. Cell host & microbe *16*, 115-127.

Lanzavecchia, A., and Sallusto, F. (2011). Ralph M. Steinman 1943–2011. Cell *147*, 1216-1217.

Lee-Kirsch, M.A., Wolf, C., Kretschmer, S., and Roers, A. (2015). Type I interferonopathies—an expanding disease spectrum of immunodysregulation. Paper presented at: Seminars in immunopathology (Springer).

Liu, K., Victora, G.D., Schwickert, T.A., Guermonprez, P., Meredith, M.M., Yao, K., Chu, F.-F., Randolph, G.J., Rudensky, A.Y., and Nussenzweig, M. (2009). In vivo analysis of dendritic cell development and homeostasis. Science *324*, 392-397.

Liu, M., Guo, S., Hibbert, J.M., Jain, V., Singh, N., Wilson, N.O., and Stiles, J.K. (2011). CXCL10/IP-10 in infectious diseases pathogenesis and potential therapeutic implications. Cytokine & growth factor reviews *22*, 121-130.

Liu, Y.-J. (2005). IPC: professional type 1 interferon-producing cells and plasmacytoid dendritic cell precursors. Annu Rev Immunol *23*, 275-306.

Loo, Y.-M., and Gale, M. (2011). Immune signaling by RIG-I-like receptors. Immunity *34*, 680-692.

Mackay, C.R. (1999). Dual personality of memory T cells. Nature *402*, 3-4.

Meixlsperger, S., Leung, C.S., Rämer, P.C., Pack, M., Vanoaica, L.D., Breton, G., Pascolo, S., Salazar, A.M., Dzionek, A., and Schmitz, J. (2013). CD141+ dendritic cells produce prominent amounts of IFN-α after dsRNA recognition and can be targeted via DEC-205 in humanized mice. Blood *121*, 5034-5044.

Messaoudi, I., Amarasinghe, G.K., and Basler, C.F. (2015). Filovirus pathogenesis and immune evasion: insights from Ebola virus and Marburg virus. Nature Reviews Microbiology *13*, 663-676.
Mohanty, S., Joshi, S.R., Ueda, I., Wilson, J., Blevins, T.P., Siconolfi, B., Meng, H., Devine, L., Raddassi, K., and Tsang, S. (2015). Prolonged proinflammatory cytokine production in monocytes modulated by interleukin 10 after influenza vaccination in older adults. Journal of Infectious Diseases *211*, 1174-1184.
Palucka, K., and Banchereau, J. (2013). Dendritic-cell-based therapeutic cancer vaccines. Immunity *39*, 38-48.
Parks, G.D., and Alexander-Miller, M.A. (2013). Paramyxovirus activation and inhibition of innate immune responses. Journal of molecular biology *425*, 4872-4892.
Pulendran, B. (2009). Learning immunology from the yellow fever vaccine: innate immunity to systems vaccinology. Nature reviews Immunology *9*, 741-747.
Pulendran, B., Oh, J.Z., Nakaya, H.I., Ravindran, R., and Kazmin, D.A. (2013). Immunity to viruses: learning from successful human vaccines. Immunological reviews *255*, 243-255.
Querec, T.D., Akondy, R.S., Lee, E.K., Cao, W., Nakaya, H.I., Teuwen, D., Pirani, A., Gernert, K., Deng, J., and Marzolf, B. (2009). Systems biology approach predicts immunogenicity of the yellow fever vaccine in humans. Nature immunology *10*, 116-125.
Rappuoli, R., Mandl, C.W., Black, S., and De Gregorio, E. (2011). Vaccines for the twenty-first century society. Nature Reviews Immunology *11*, 865-872.
Rehwinkel, J., and e Sousa, C.R. (2013). Targeting the viral Achilles' heel: recognition of 5′-triphosphate RNA in innate anti-viral defence. Current opinion in microbiology *16*, 485-492.
Reizis, B., Bunin, A., Ghosh, H.S., Lewis, K.L., and Sisirak, V. (2011). Plasmacytoid dendritic cells: recent progress and open questions. Annual review of immunology *29*, 163.
Rothenfusser, S., Goutagny, N., DiPerna, G., Gong, M., Monks, B.G., Schoenemeyer, A., Yamamoto, M., Akira, S., and Fitzgerald, K.A. (2005). The RNA helicase Lgp2 inhibits TLR-independent sensing of viral replication by retinoic acid-inducible gene-I. The Journal of Immunology *175*, 5260-5268.
Sakaguchi, S., Vignali, D.A., Rudensky, A.Y., Niec, R.E., and Waldmann, H. (2013). The plasticity and stability of regulatory T cells. Nature Reviews Immunology *13*, 461-467.
Sato, S., Li, K., Kameyama, T., Hayashi, T., Ishida, Y., Murakami, S., Watanabe, T., Iijima, S., Sakurai, Y., and Watashi, K. (2015). The RNA sensor RIG-I dually functions as an innate sensor and direct antiviral factor for hepatitis B virus. Immunity *42*, 123-132.
Satoh, T., Kato, H., Kumagai, Y., Yoneyama, M., Sato, S., Matsushita, K., Tsujimura, T., Fujita, T., Akira, S., and Takeuchi, O. (2010). LGP2 is a positive regulator of RIG-I–and MDA5-mediated antiviral responses. Proceedings of the National Academy of Sciences *107*, 1512-1517.
Scherer, C.A., Magness, C.L., Steiger, K.V., Poitinger, N.D., Caputo, C.M., Miner, D.G., Winokur, P.L., Klinzman, D., McKee, J., and Pilar, C. (2007). Distinct gene expression profiles in peripheral blood mononuclear cells from patients infected with vaccinia virus, yellow fever 17D virus, or upper respiratory infections. Vaccine *25*, 6458-6473.
Schlee, M. (2013). Master sensors of pathogenic RNA–RIG-I like receptors. Immunobiology *218*, 1322-1335.

Sedger, L.M. (2013). microRNA control of interferons and interferon induced anti-viral activity. Molecular immunology *56*, 781-793.
Seth, R.B., Sun, L., Ea, C.-K., and Chen, Z.J. (2005). Identification and characterization of MAVS, a mitochondrial antiviral signaling protein that activates NF-κB and IRF3. Cell *122*, 669-682.
Shakhar, G., Lindquist, R.L., Skokos, D., Dudziak, D., Huang, J.H., Nussenzweig, M.C., and Dustin, M.L. (2005). Stable T cell–dendritic cell interactions precede the development of both tolerance and immunity in vivo. Nature immunology *6*, 707-714.
Shen, P., and Fillatreau, S. (2015). Antibody-independent functions of B cells: a focus on cytokines. Nature Reviews Immunology.
Shortman, K., and Liu, Y.-J. (2002). Mouse and human dendritic cell subtypes. Nature Reviews Immunology *2*, 151-161.
Skaug, B., and Chen, Z.J. (2010). Emerging role of ISG15 in antiviral immunity. Cell *143*, 187-190.
Steinman, R.M. (2012). Decisions about dendritic cells: past, present, and future. Annual review of immunology *30*, 1-22.
Stuart, L.M., Paquette, N., and Boyer, L. (2013). Effector-triggered versus pattern-triggered immunity: how animals sense pathogens. Nature Reviews Immunology *13*, 199-206.
Swiecki, M., and Colonna, M. (2015). The multifaceted biology of plasmacytoid dendritic cells. Nature Reviews Immunology *15*, 471-485.
Trumpfheller, C., Longhi, M.P., Caskey, M., Idoyaga, J., Bozzacco, L., Keler, T., Schlesinger, S.J., and Steinman, R.M. (2012). Dendritic cell- targeted protein vaccines: a novel approach to induce T- cell immunity. Journal of internal medicine *271*, 183-192.
van Kempen, T.S., Wenink, M.H., Leijten, E.F., Radstake, T.R., and Boes, M. (2015). Perception of self: distinguishing autoimmunity from autoinflammation. Nature Reviews Rheumatology.
Verhelst, J., Parthoens, E., Schepens, B., Fiers, W., and Saelens, X. (2012). Interferon-inducible protein Mx1 inhibits influenza virus by interfering with functional viral ribonucleoprotein complex assembly. Journal of virology *86*, 13445-13455.
Williams, D.W., Veenstra, M., Gaskill, P.J., Morgello, S., Calderon, T.M., and Berman, J.W. (2014). Monocytes mediate HIV neuropathogenesis: mechanisms that contribute to HIV associated neurocognitive disorders. Current HIV research *12*, 85.
Wu, B., and Hur, S. (2015). How RIG-I like receptors activate MAVS. Current opinion in virology *12*, 91-98.
Yoneyama, M., Kikuchi, M., Natsukawa, T., Shinobu, N., Imaizumi, T., Miyagishi, M., Taira, K., Akira, S., and Fujita, T. (2004). The RNA helicase RIG-I has an essential function in double-stranded RNA-induced innate antiviral responses. Nature immunology *5*, 730-737.
Zhang, Z., Cheng, L., Zhao, J., Li, G., Zhang, L., Chen, W., Nie, W., Reszka-Blanco, N.J., Wang, F.-S., and Su, L. (2015). Plasmacytoid dendritic cells promote HIV-1–induced group 3 innate lymphoid cell depletion. The Journal of clinical investigation *125*, 0-0.
Zhu, F.X., King, S.M., Smith, E.J., Levy, D.E., and Yuan, Y. (2002). A Kaposi's sarcoma-associated herpesviral protein inhibits virus-mediated induction of type I interferon by blocking IRF-7 phosphorylation and nuclear accumulation. Proceedings of the National Academy of Sciences *99*, 5573-5578.

Ziegler-Heitbrock, L. (2007). The CD14+ CD16+ blood monocytes: their role in infection and inflammation. Journal of leukocyte biology *81*, 584-592.
Ziegler-Heitbrock, L. (2015). Blood monocytes and their subsets: established features and open questions. Frontiers in immunology *6*.
Zitvogel, L., Galluzzi, L., Kepp, O., Smyth, M.J., and Kroemer, G. (2015). Type I interferons in anticancer immunity. Nature Reviews Immunology *15*, 405-414.

ACKNOWLEDGEMENTS

First of all, I want to express my appreciation to Prof. Dr. med. Anne Krug, who provided me with the opportunity to pursue my doctoral thesis in her laboratory. I want to thank her for her guidance and constructive criticism, especially throughout the writing process.

I am grateful to Dr. rer. nat. Katharina Eisenächer for being a great teacher, for her support, advice and most importantly for her friendship.

I also want to specifically thank Dr. rer. nat. Alexander Heiseke for sharing his expertise in FACS analyses, qRT-PCR and his patience in answering all my questions.

Furthermore, I want to express my gratitude to all lab members of the AG Krug for their support and help whenever needed.

Special thanks to my dear friend Sasha, who taught me to speak English freely and who has opened my eyes to the world.

I am most grateful to my family, my parents, my sister and grandmother for always standing by my side, for their encouragement, love and support. Without them, this would have been neither possible nor worth it. Thank you! I love you!

DECLARATION OF HONOUR

I hereby confirm that I have composed and written this dissertation by myself and have acknowledged all additional assistance within the work. I am familiar with the relevant course of examination for doctoral candidates and have followed its instructions.

Munich, 18.01.2016

Livia Habenicht